

Electronic Supplementary Information (ESI)

Preparation and ion recognition features of porphyrin-chalcone type compounds as efficient red-fluorescent materials

Nuno M. M. Moura,^{a,b,c} Cristina Núñez,^{*b,d,e} M. Amparo F. Faustino,^a José A. S. Cavaleiro,^a M. Graça P. M. S. Neves,^{*a} José Luis Capelo,^{b,c} Carlos Lodeiro^{*b,c}

^a Chemistry Department and QOPNA, University of Aveiro, Campus Universitário Santiago, 3810-193 Aveiro, Portugal.

^b BIOSCOPE Group, REQUIMTE-CQFB, Chemistry Department, Faculty of Science and Technology, University NOVA of Lisbon, 2829-516 Monte de Caparica, Portugal.

^c ProteoMass Scientific Society. Madan Parque. Rua dos Inventores. 2825-182. Caparica. Portugal.

^d Ecology Research Group, Department of Geographical and Life Sciences, Canterbury Christ Church University, CT1 1QU Canterbury, United Kingdom.

^e Inorganic Chemistry Department, Faculty of Chemistry, University of Santiago de Compostela, 15782 Santiago de Compostela, Spain

Table of Contents

I - NMR and IV spectra

II - Photophysical characterization data

III - Metal ion titrations data

IV - NMR titrations

V - MALDI-TOF-MS titrations data

I - NMR and IV spectra

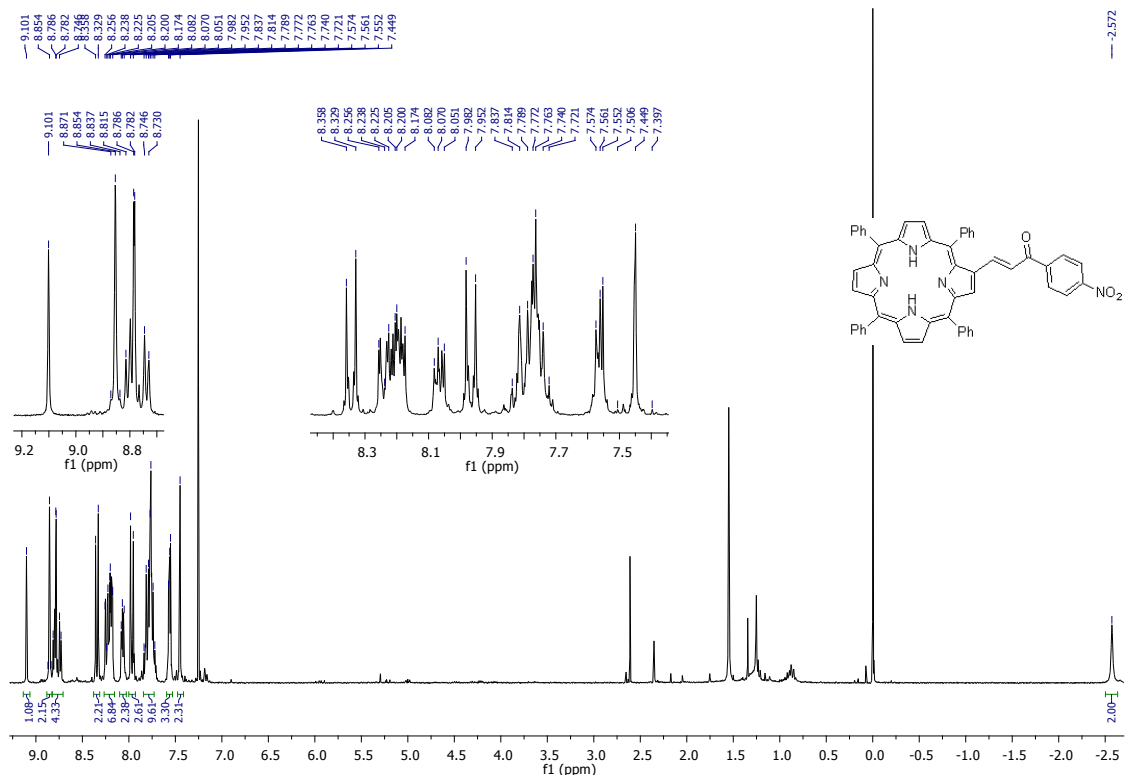


Figure 1_S_M - ^1H NMR spectrum of compound **4a**.

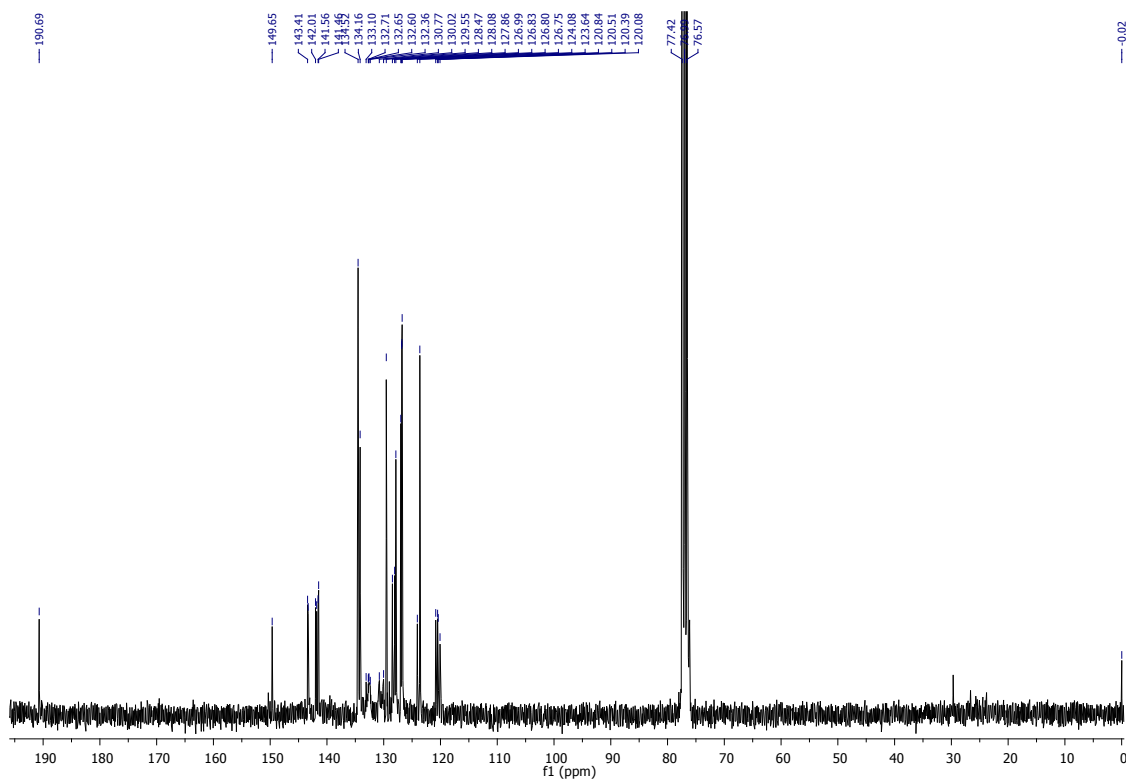


Figure 2-SM - ^{13}C NMR spectrum of compound **4a**.

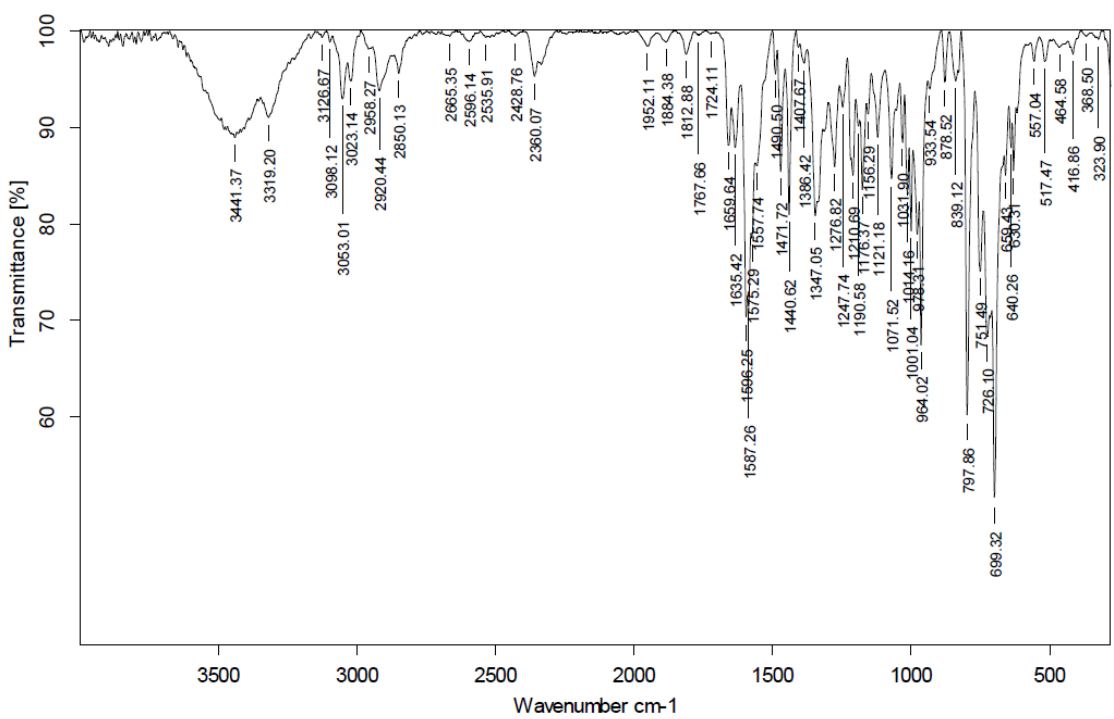


Figure 3_SM - Infra-red spectrum of compound 4a.

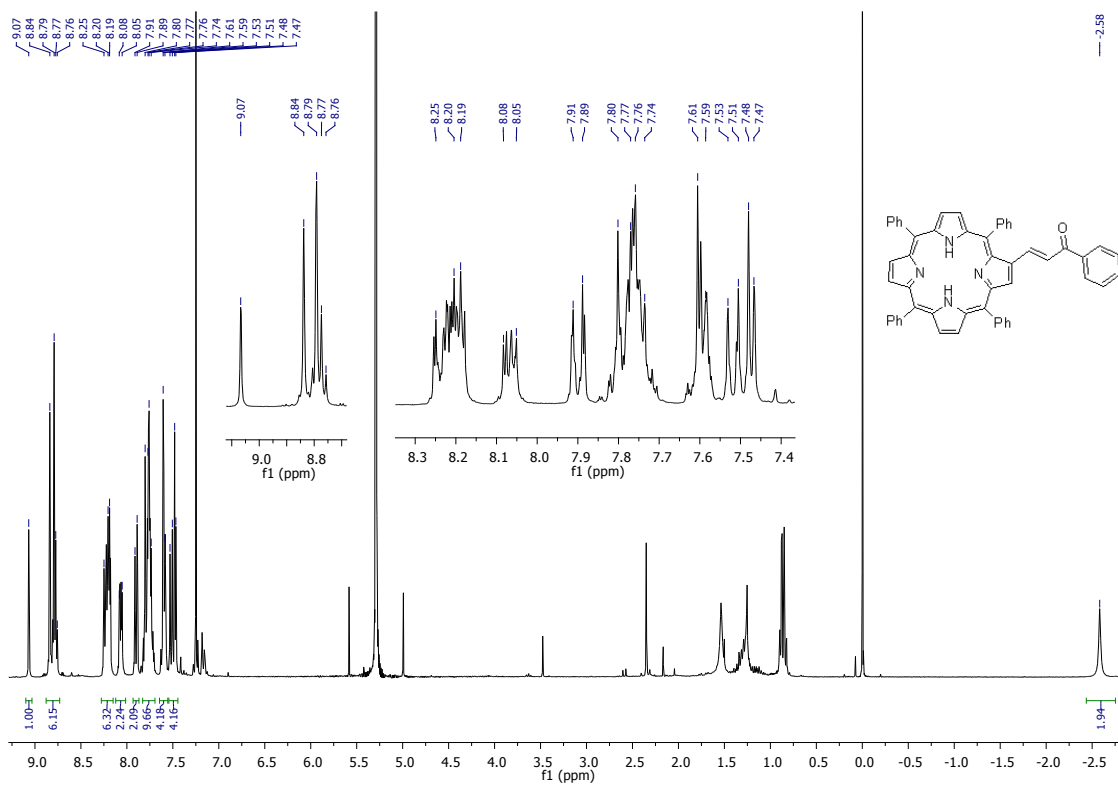


Figure 4_SM - ^1H NMR spectrum of compound 4b.

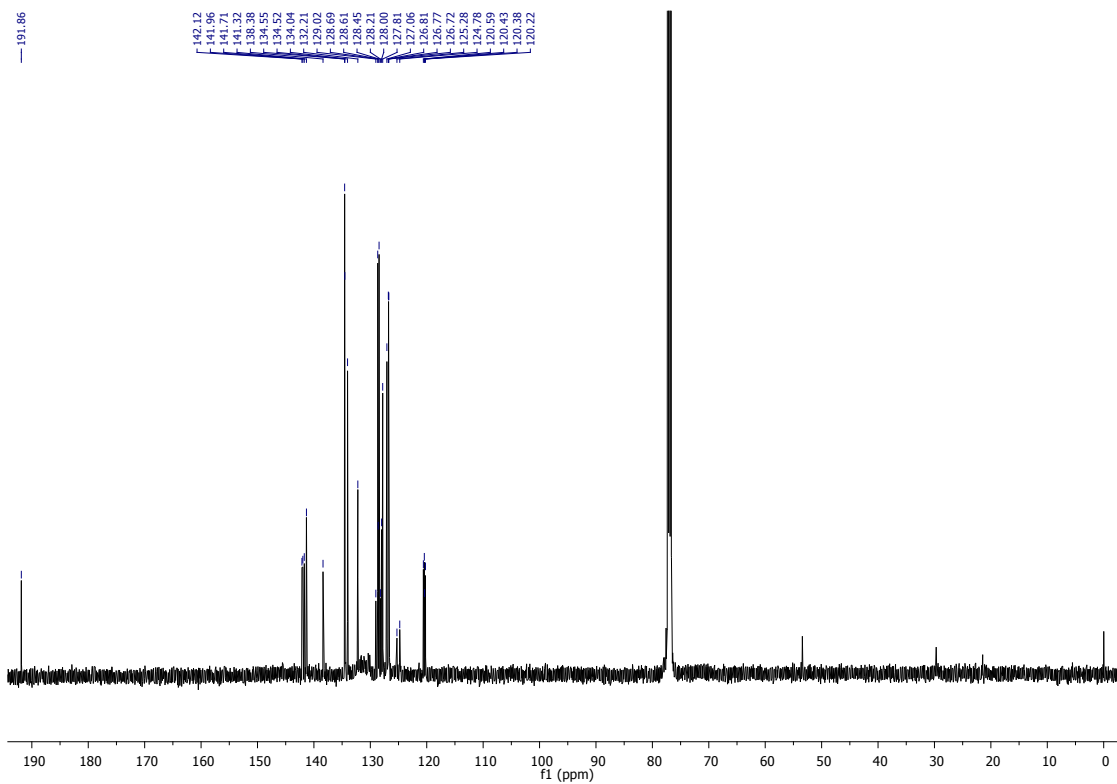


Figure 5_SM - ^{13}C NMR spectrum of compound **4b.**

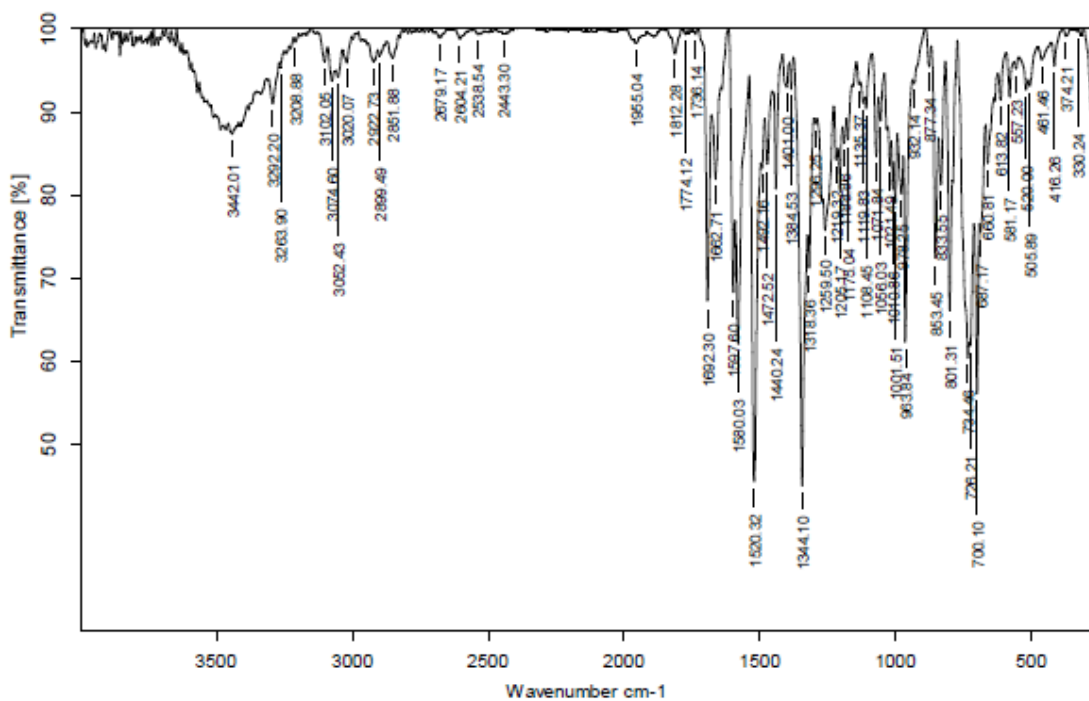


Figure 6_SM - Infra-red spectrum of compound **4b.**

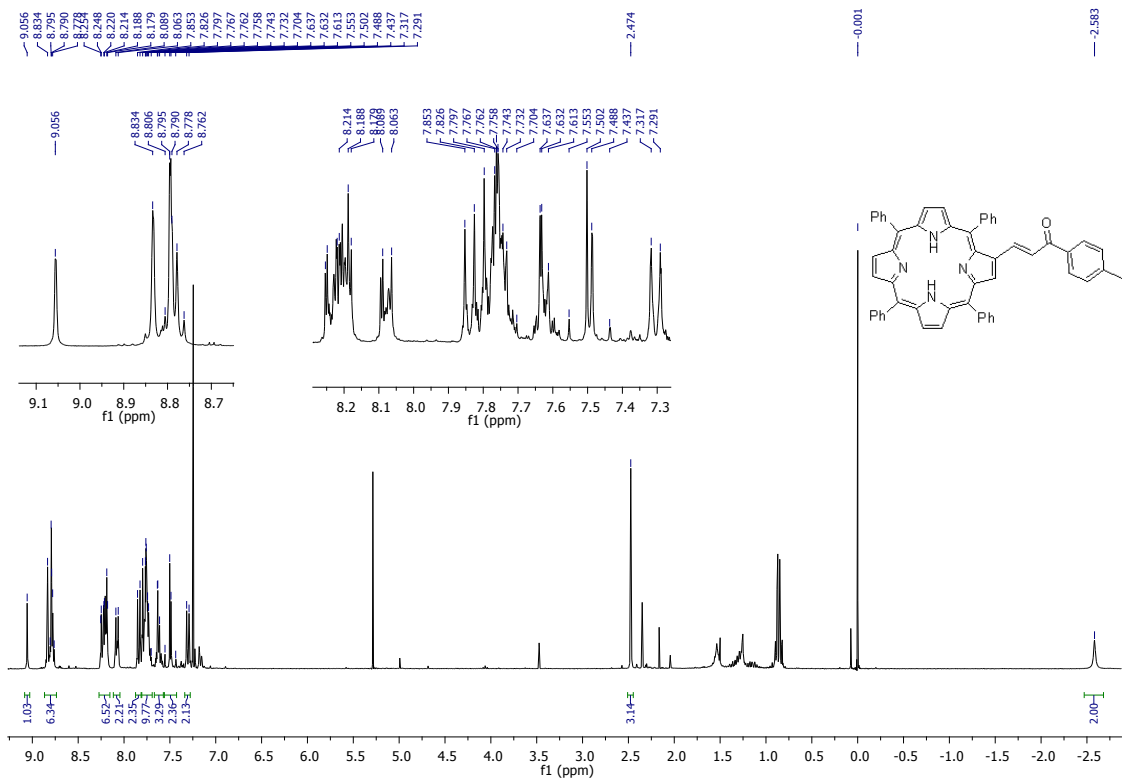


Figure 7_SM - ^1H NMR spectrum of compound 4c.

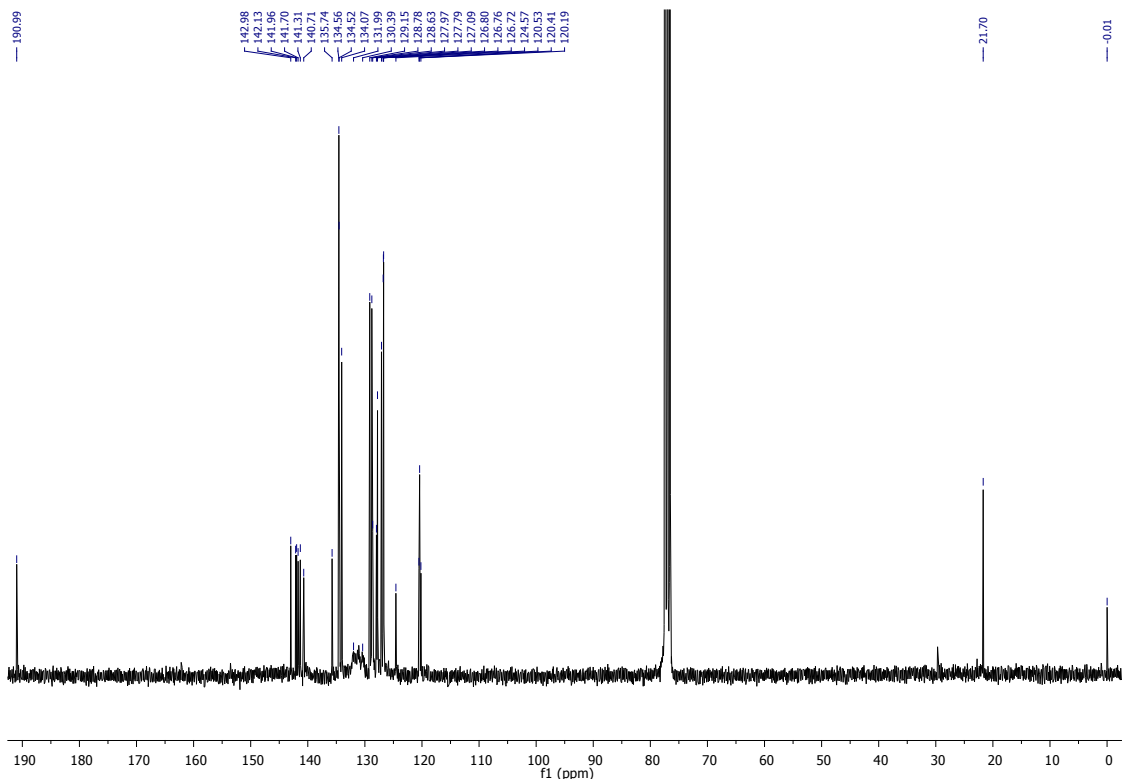


Figure 8_S_M - ^{13}C NMR spectrum of compound **4c**.

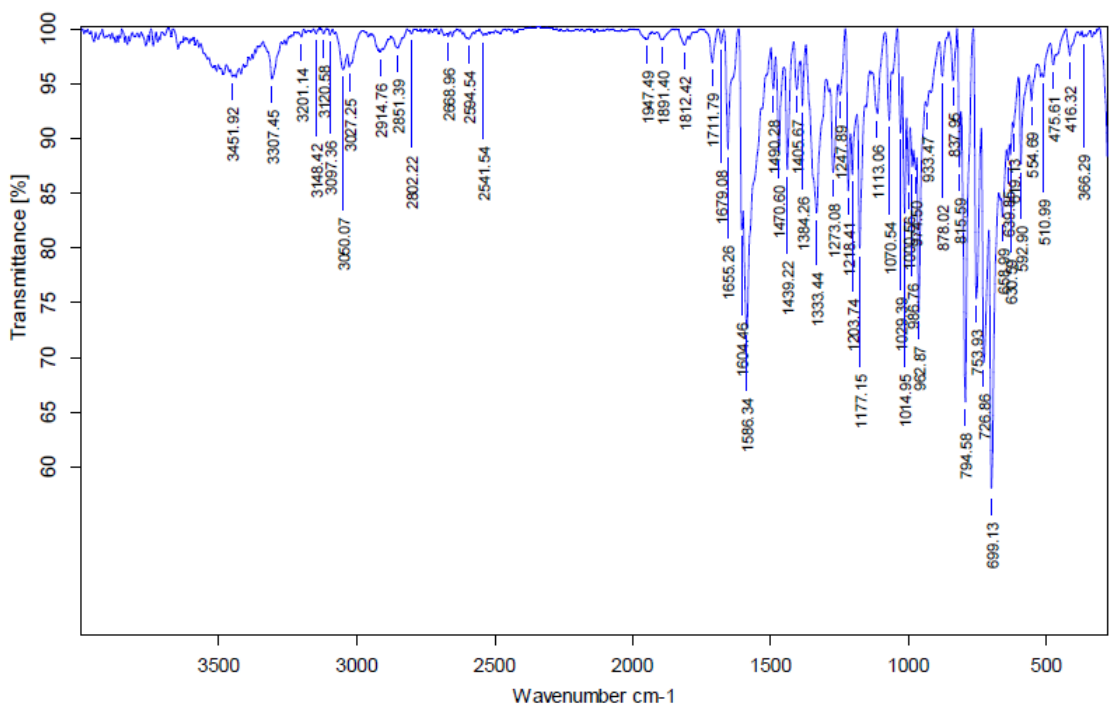


Figure 9_SM - Infra-red spectrum of compound 4c.

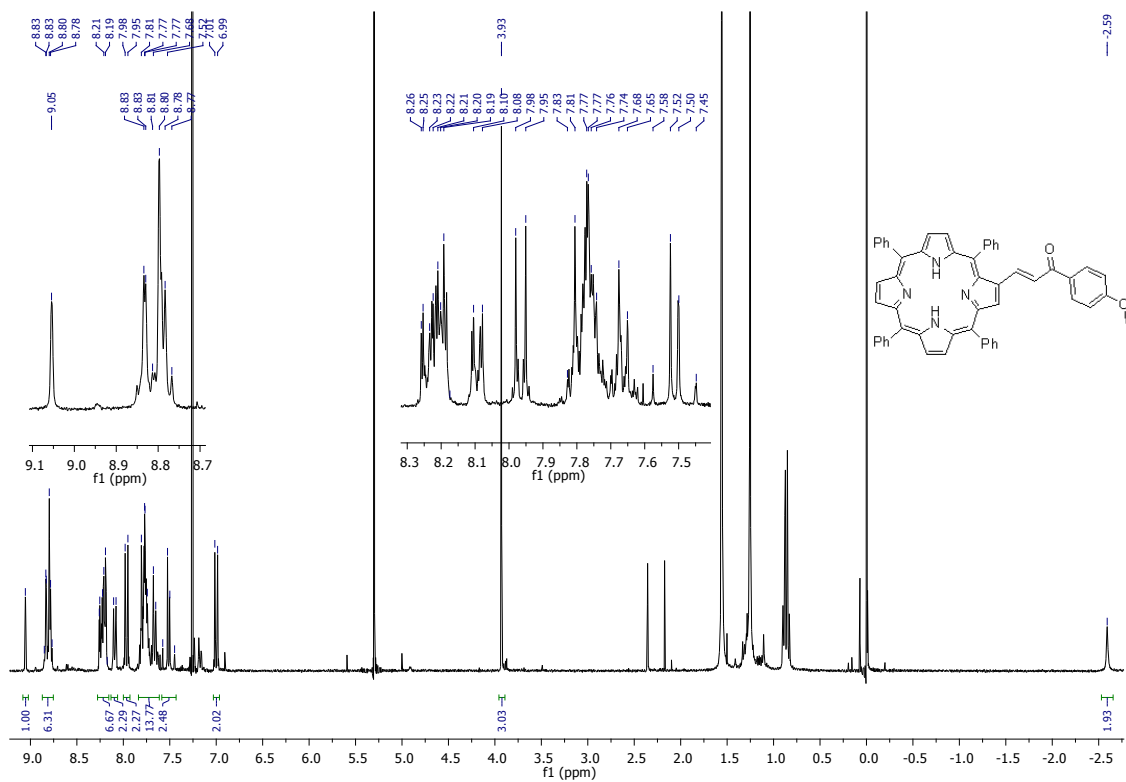


Figure 10_SM – ^1H NMR spectrum of compound 4d.

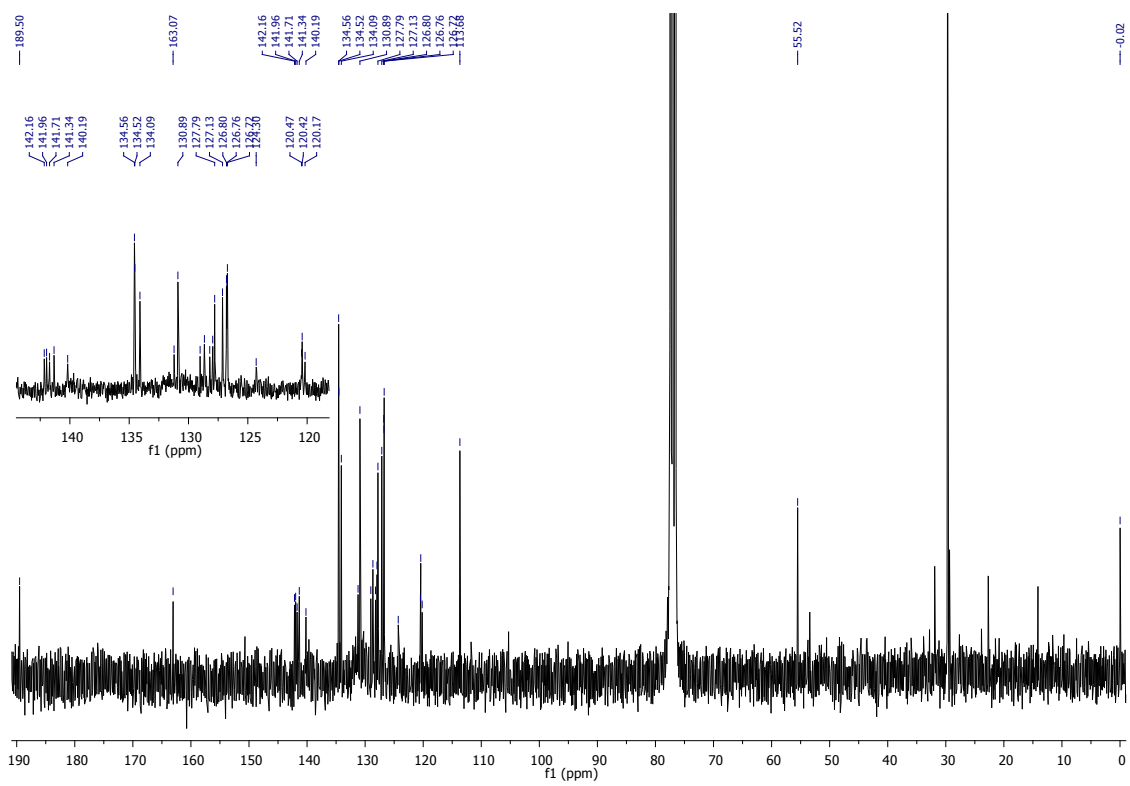


Figure 11_SM - ^{13}C NMR spectrum of compound 4d.

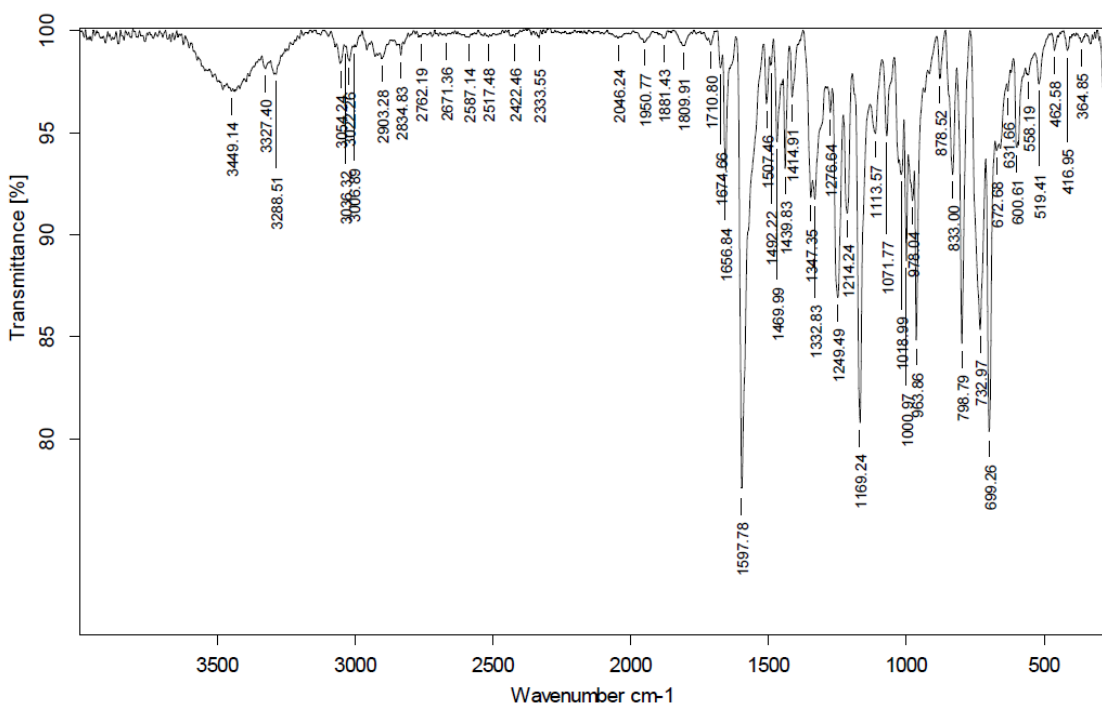


Figure 12_SM - Infra-red spectrum of compound 4d.

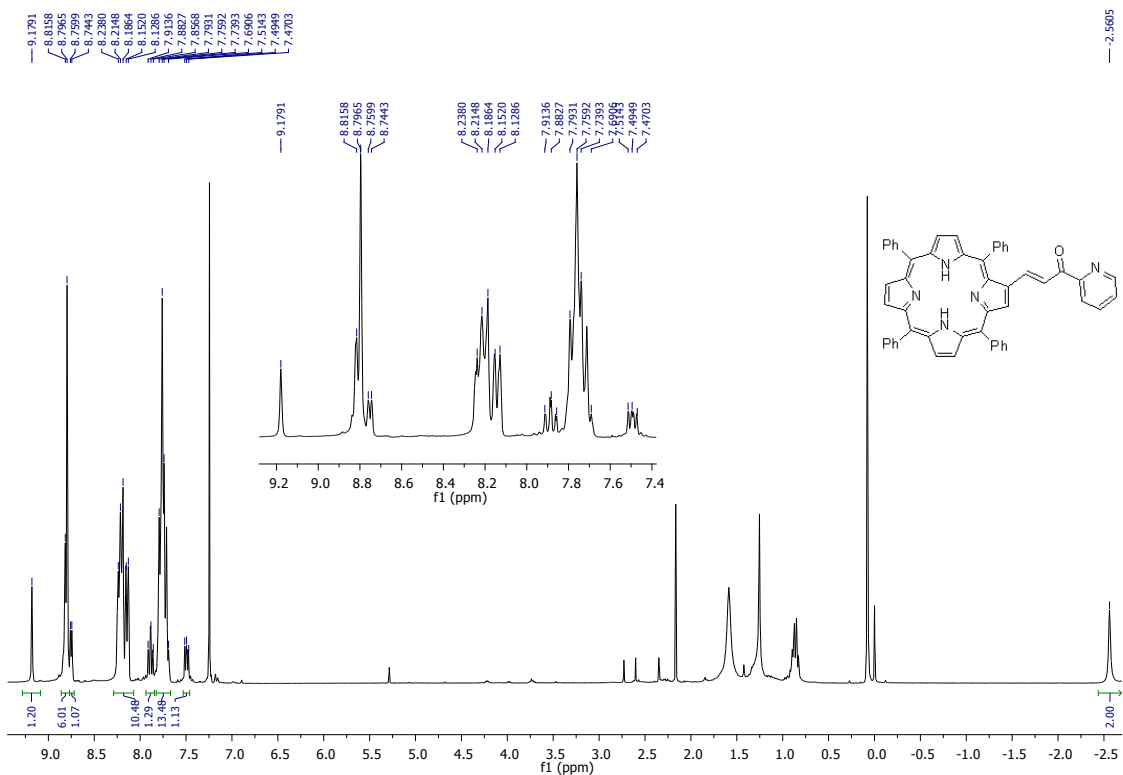


Figure 13_SM - ^1H NMR spectrum of compound **4e**.

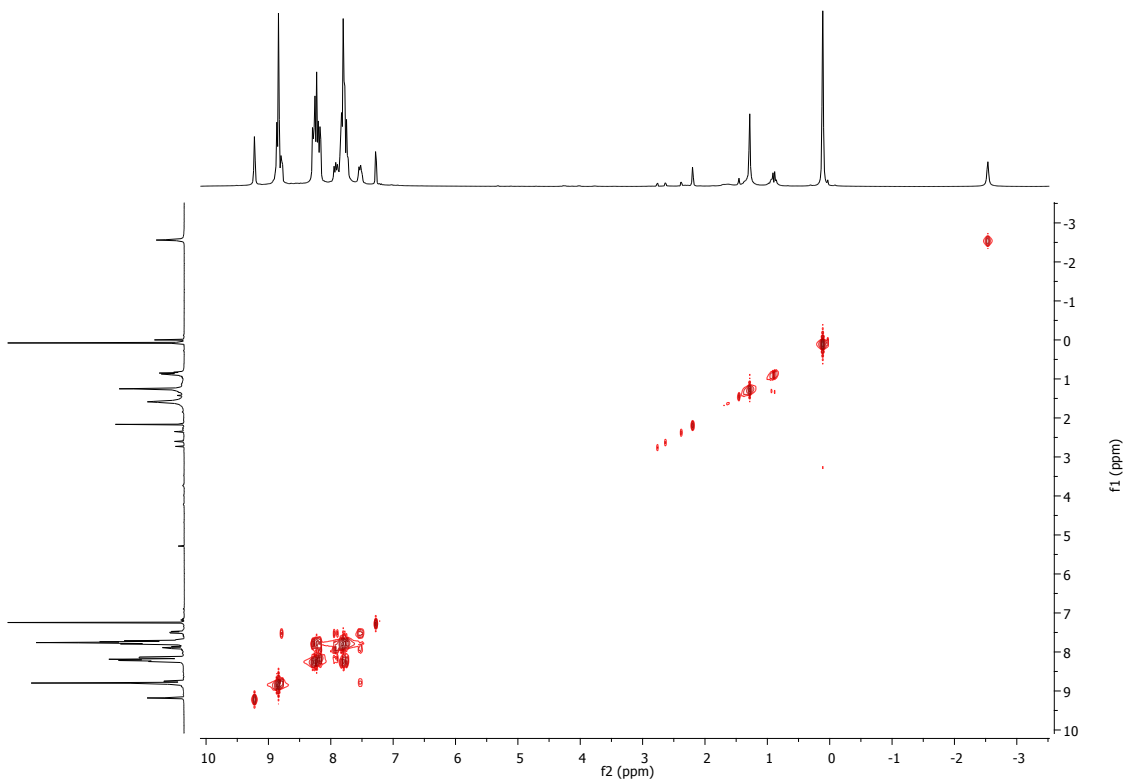


Figure 14_SM – COSY spectrum of compound 4e.

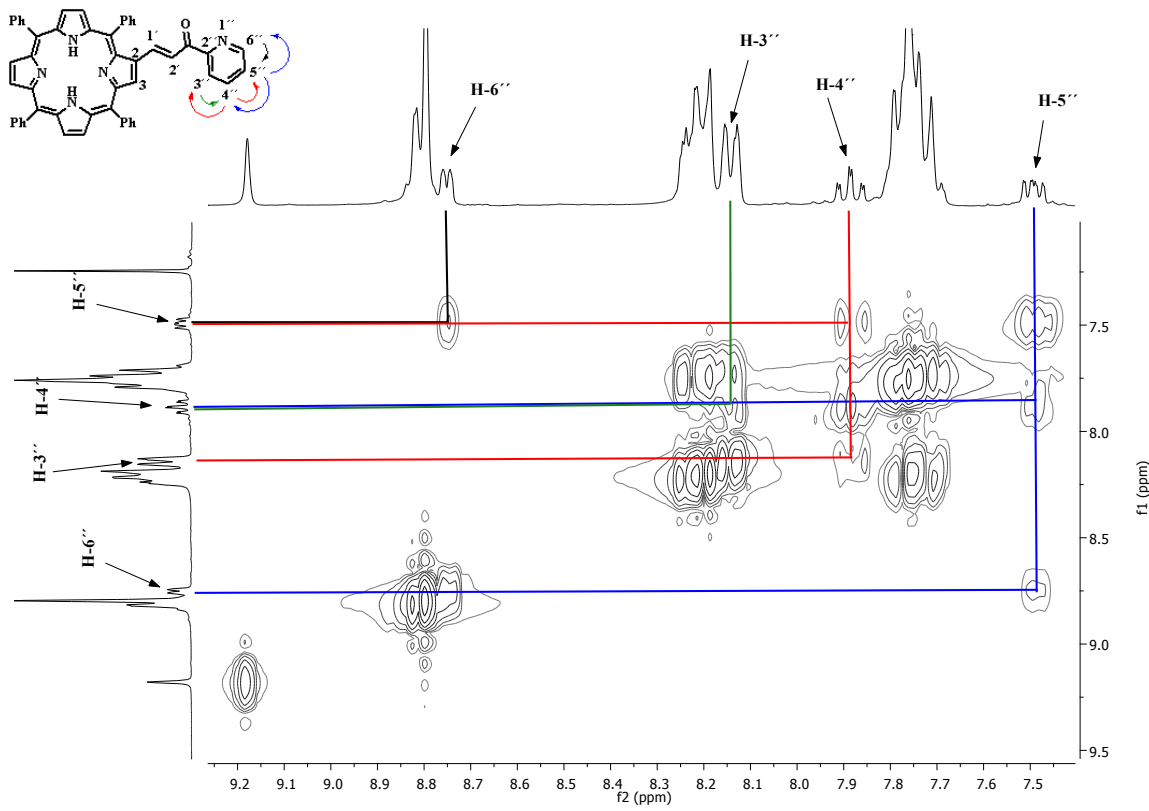


Figure 15_SM – Partial COSY spectrum of compound 4e.

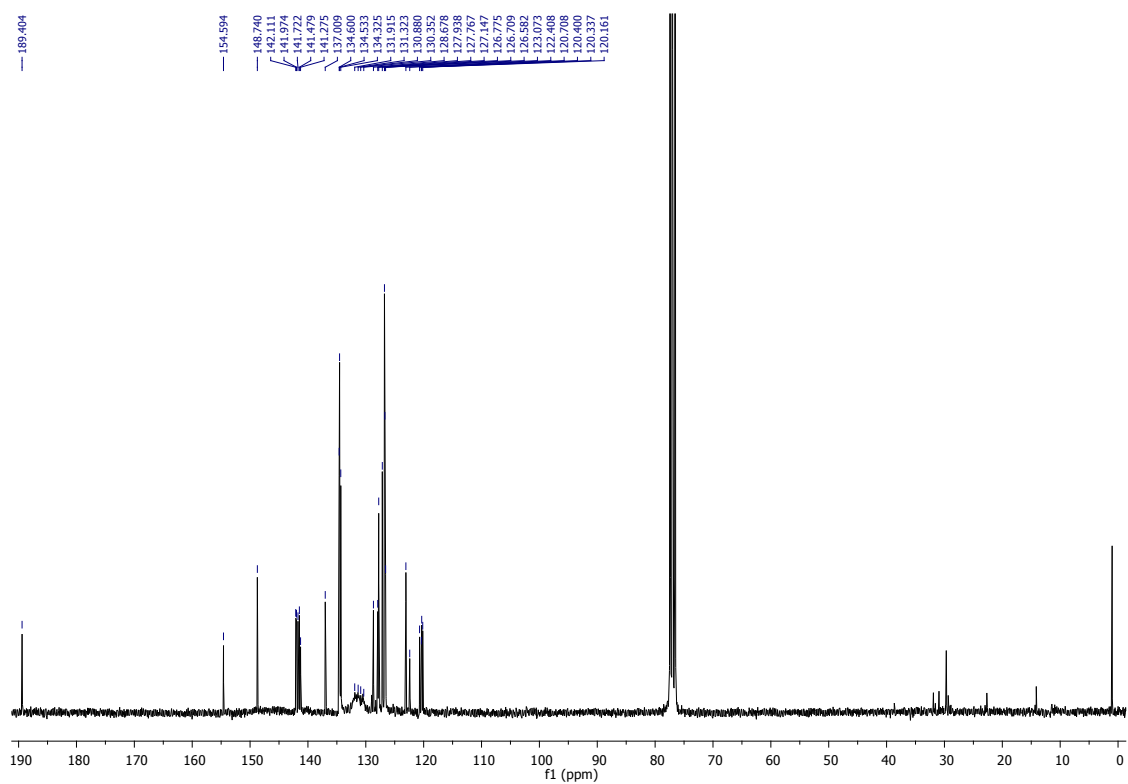


Figure 16_SM – ^{13}C NMR spectrum of compound 4e.

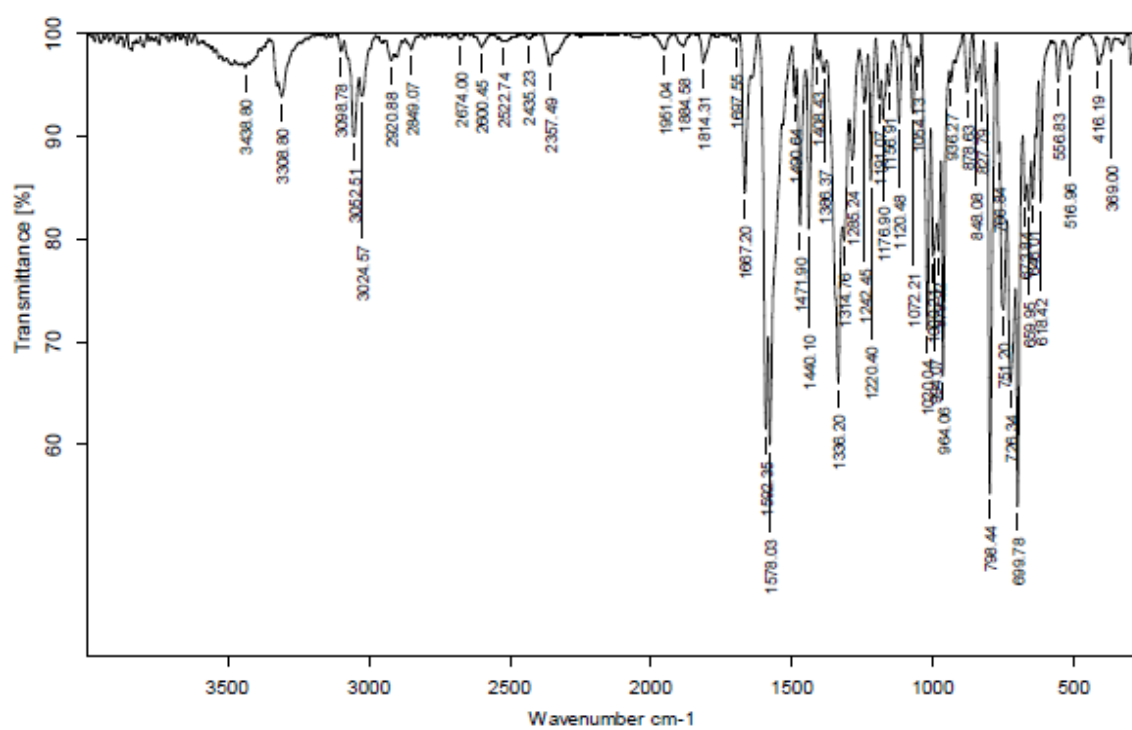


Figure 17_SM - Infra-red spectrum of compound 4e.

II - Photophysical characterization data

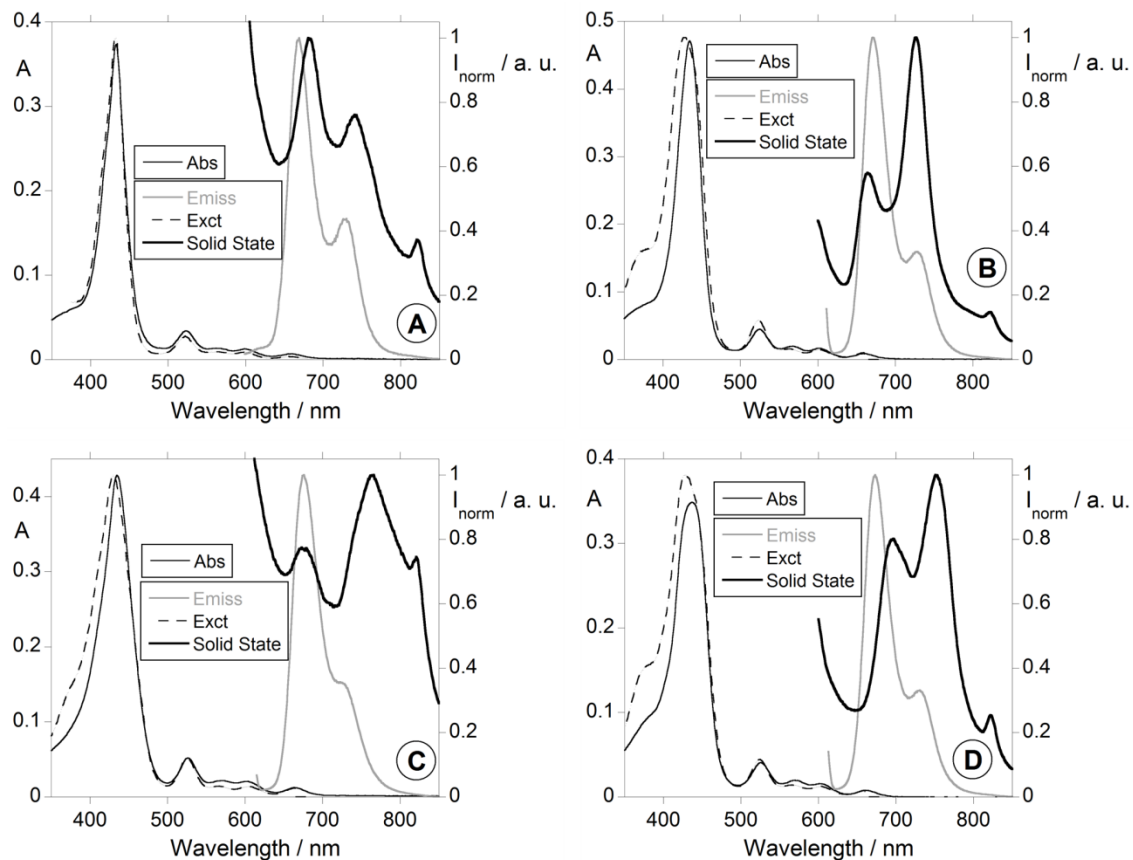


Figure 18_SM - Absorption and normalized emission and excitation of compounds **4a** (A), **4b** (B), **4d** (C) and **4e** (D) in CHCl_3 ($[4\mathbf{a}] = [4\mathbf{b}] = [4\mathbf{d}] = [4\mathbf{e}] = 2.50 \times 10^{-6} \text{ M}$, $\lambda_{\text{exc}4\mathbf{a}} = 602 \text{ nm}$ and $\lambda_{\text{emiss}4\mathbf{a}} = 728 \text{ nm}$; $\lambda_{\text{exc}4\mathbf{b}} = 599 \text{ nm}$ and $\lambda_{\text{emiss}4\mathbf{b}} = 728 \text{ nm}$; $\lambda_{\text{exc}4\mathbf{d}} = 601 \text{ nm}$ and $\lambda_{\text{emiss}4\mathbf{c}} = 727 \text{ nm}$; $\lambda_{\text{exc}4\mathbf{e}} = 603 \text{ nm}$ and $\lambda_{\text{emiss}4\mathbf{e}} = 731 \text{ nm}$) and emission of spectra in solid state at room temperature.

III - Metal ion titrations data

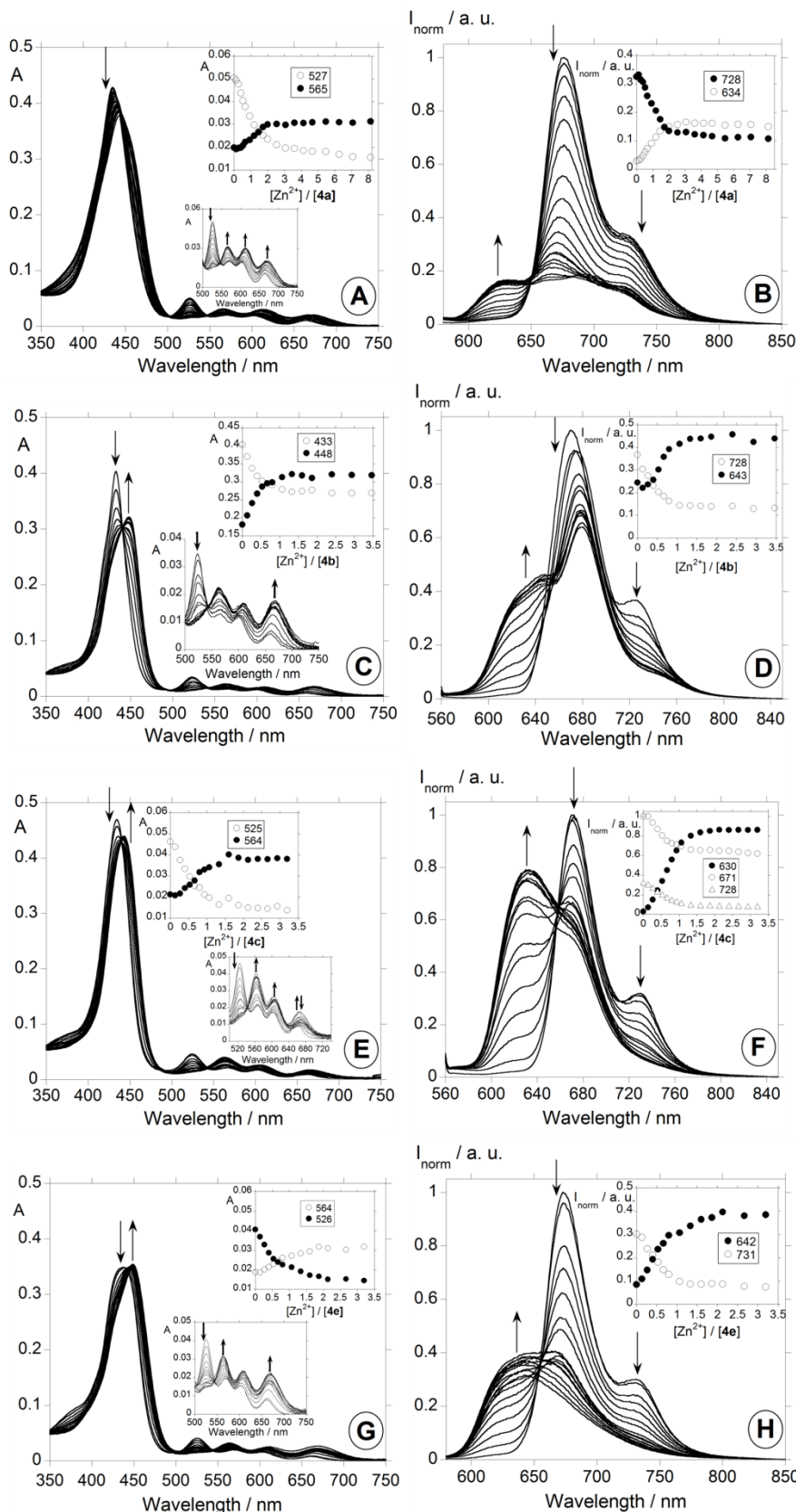


Figure 19_SM – Spectrophotometric (A, C, E and G) and spectrofluorimetric (B, D, F and H) titrations of compounds **4a, **4b**, **4c** and **4e** in chloroform as a function of added Zn^{2+} in acetonitrile. The insets show the absorption at 527 and 565 nm (A), 433 and 448 nm (C), 525 and 564 nm (E) and 526 and 564 nm (G); and the normalized fluorescence intensity at 634 and 728 nm (B), 643 and 728 nm (D), 630, 671 and 728 nm (F) and 642 and 731 nm (H) ($[4a] = [4b] = [4c] = [4e] = 2.50 \times 10^{-6} M$; $\lambda_{exc4a} = 548$ nm, $\lambda_{exc4b} = 542$ nm, $\lambda_{exc4c} = 545$ nm, $\lambda_{exc4e} = 545$ nm).**

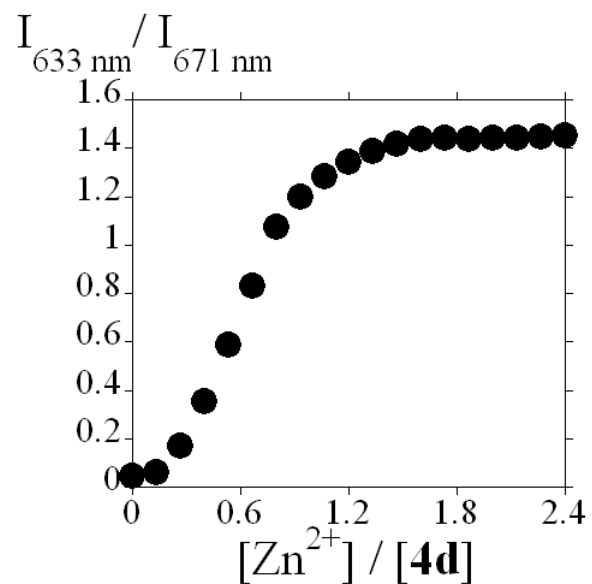


Figure 20_SM - Ratio ($I_{\text{norm}(633\text{nm})}/I_{\text{norm}(671\text{ nm})}$) changes as a function of the Zn^{2+} concentration.

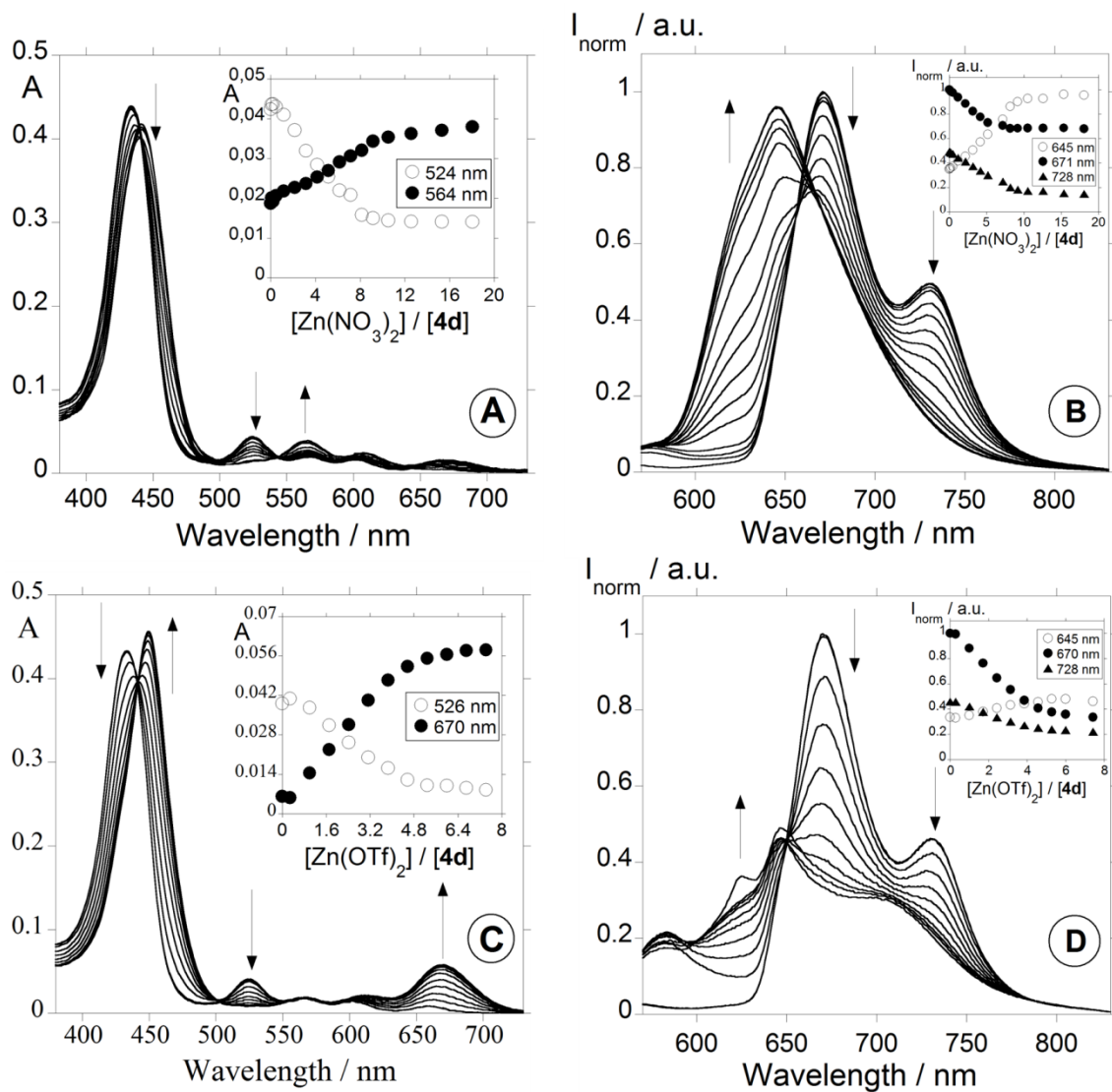


Figure 21_SM – Spectrophotometric (**A** and **C**) and spectrofluorimetric (**B** and **D**) titrations of compound **4d** in chloroform as a function of added $\text{Zn}(\text{NO}_3)_2$ and $\text{Zn}(\text{OTf})_2$ in acetonitrile. The insets show the absorption at 524 and 564 nm (**A**) and 526 and 670 nm (**C**); and the normalized fluorescence intensity at 645, 671 and 728 nm (**B** and **C**) ($[4\mathbf{d}] = 2.50 \times 10^{-6} \text{ M}$, $\lambda_{\text{exc}4\mathbf{d}} = 549 \text{ nm}$).

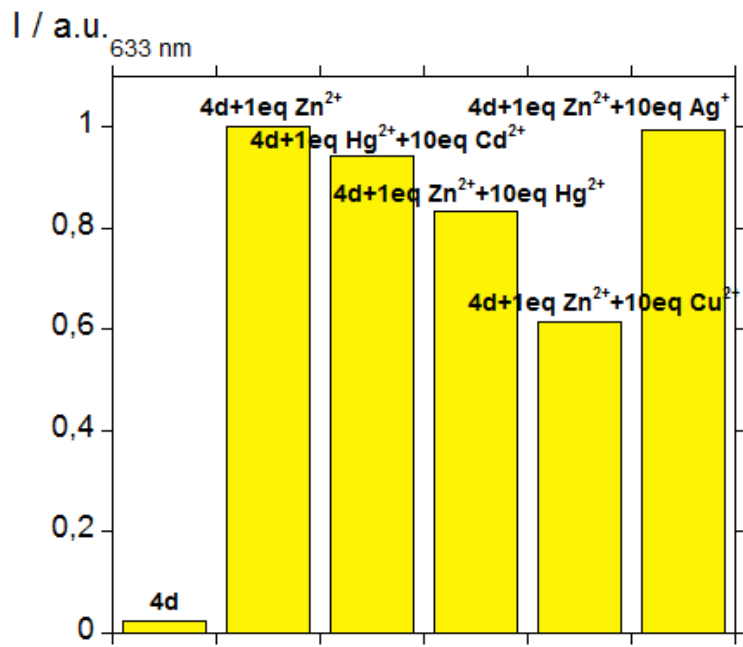


Figure 22_SM - Comparative fluorescence response of chemosensor **4d** ($2.50 \times 10^{-6} \text{ M}$, $\lambda_{\text{exc}4d} = 549 \text{ nm}$) to Cu^{2+} , Hg^{2+} , Cd^{2+} and Ag^+ (10 equiv.) in chloroform after the addition of $\text{Zn}(\text{BF}_4)_2 \cdot \text{xH}_2\text{O}$ (1 equiv.).

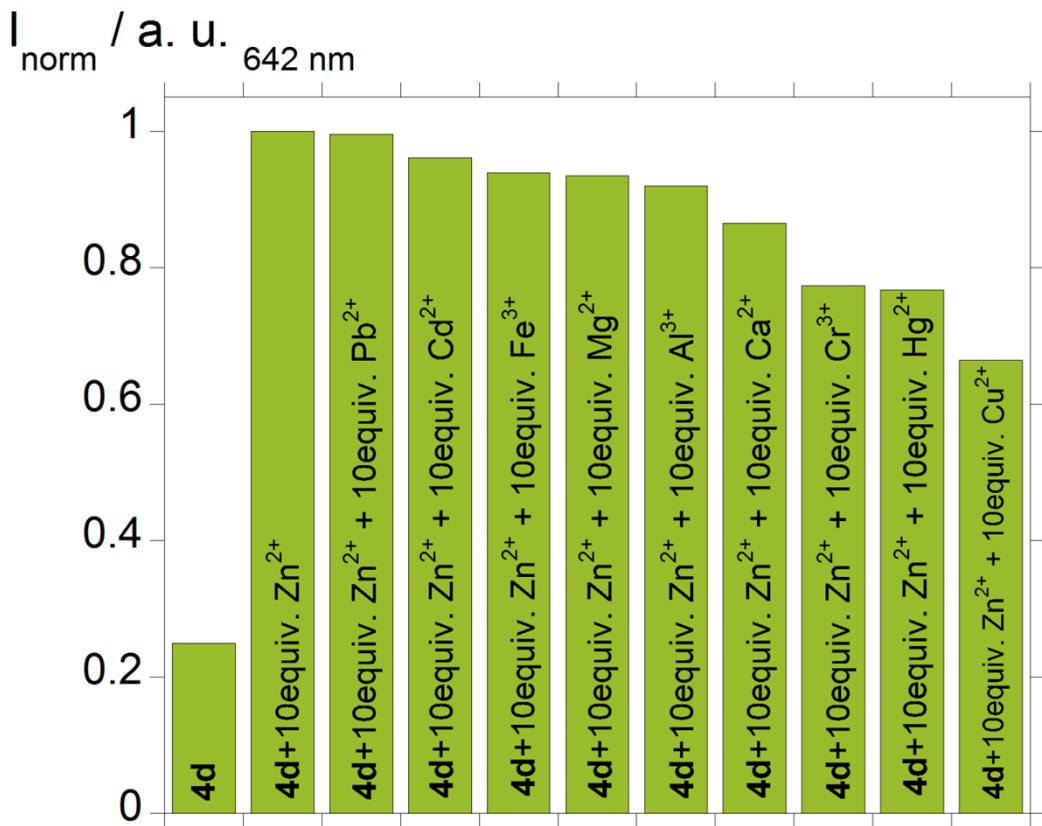


Figure 23_SM - Comparative fluorescence response of chemosensor **4d** ($2.50 \times 10^{-6} \text{ M}$, $\lambda_{\text{exc}4d} = 549 \text{ nm}$) to Pb^{2+} , Cd^{2+} , Fe^{3+} , Mg^{2+} , Al^{3+} , Ca^{2+} , Cr^{3+} , Hg^{2+} , and Cu^{2+} (10 equiv.) after the addition of $\text{Zn}(\text{NO}_3)_2 \cdot \text{xH}_2\text{O}$ (10 equiv.).

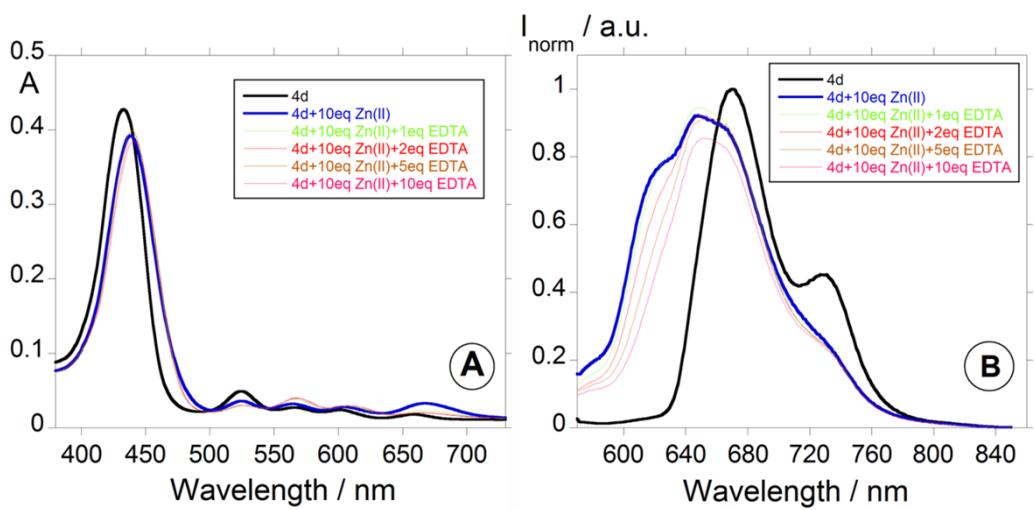


Figure 24_SM - Comparative absorption and fluorescence response of chemosensor **4d in chloroform (2.50 \times 10⁻⁶ M, $\lambda_{\text{exc}4d}$ = 549 nm) to 1, 2, 5 and 10 equiv. of ethylenediaminetetraacetic acid (EDTA) in acetonitrile after the addition of Zn²⁺ (10 equiv.) in acetonitrile.**

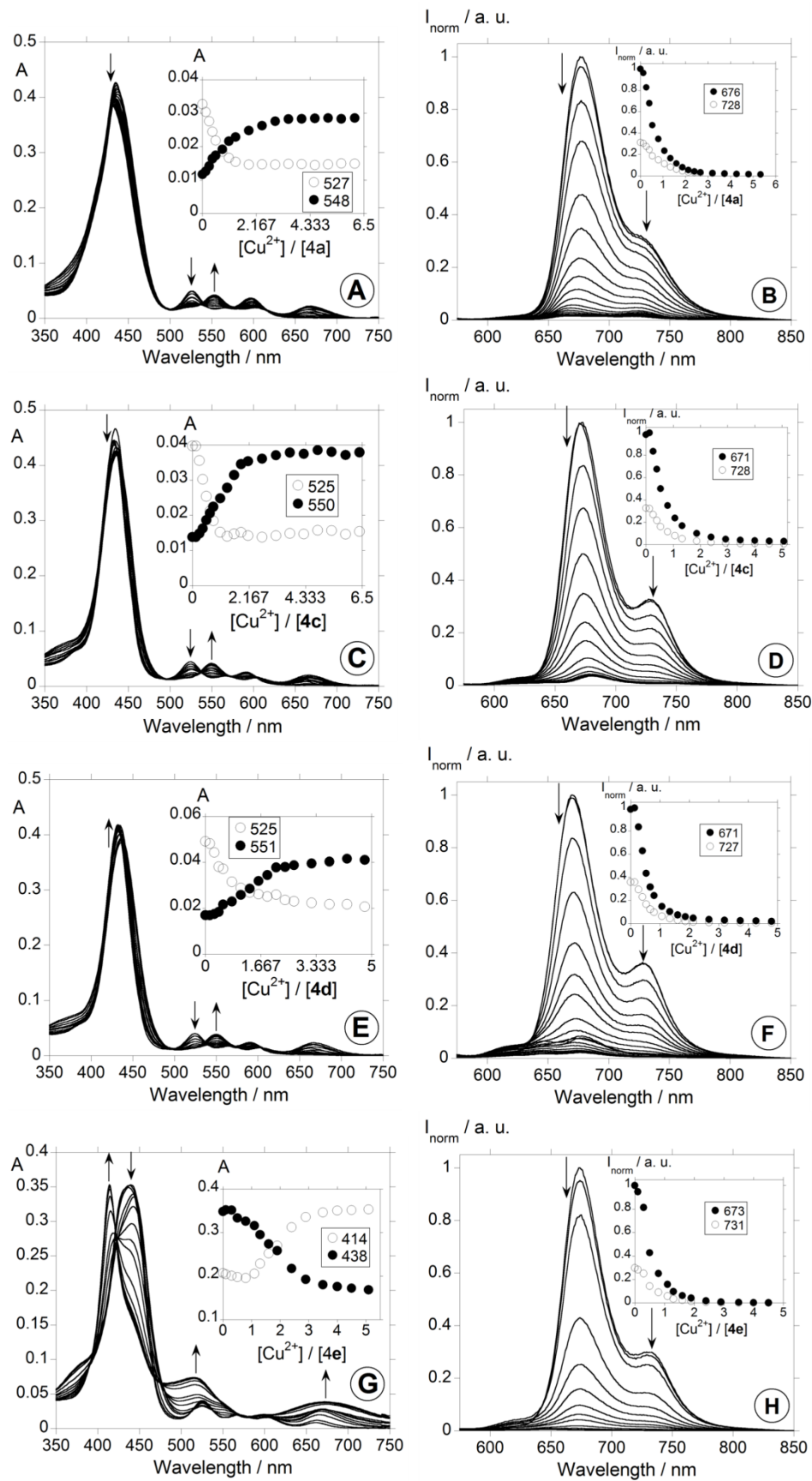


Figure 25_SM - Spectrophotometric (A, C, E and G) and spectrofluorimetric (B, D, F and H) titrations of compounds **4a, **4c**, **4d** and **4e** in chloroform as a function of added Cu^{2+} in acetonitrile. The insets show the absorption at 527 and 548 nm (A), 525 and 550 nm (C), 525 and 551 nm (E) and 414 and 438 nm (G); and the normalized fluorescence intensity at 676 and 728 nm (B), 676 and 728 nm (D), 671 and 728 nm (F) and 673 and 731 nm (H) ($[4a] = [4c] = [4d] = [4e] = 2.50 \times 10^{-6} M$; $\lambda_{exc4a} = 548$ nm, $\lambda_{exc4c} = 545$ nm, $\lambda_{exc4d} = 549$ nm, $\lambda_{exc4e} = 545$ nm).**

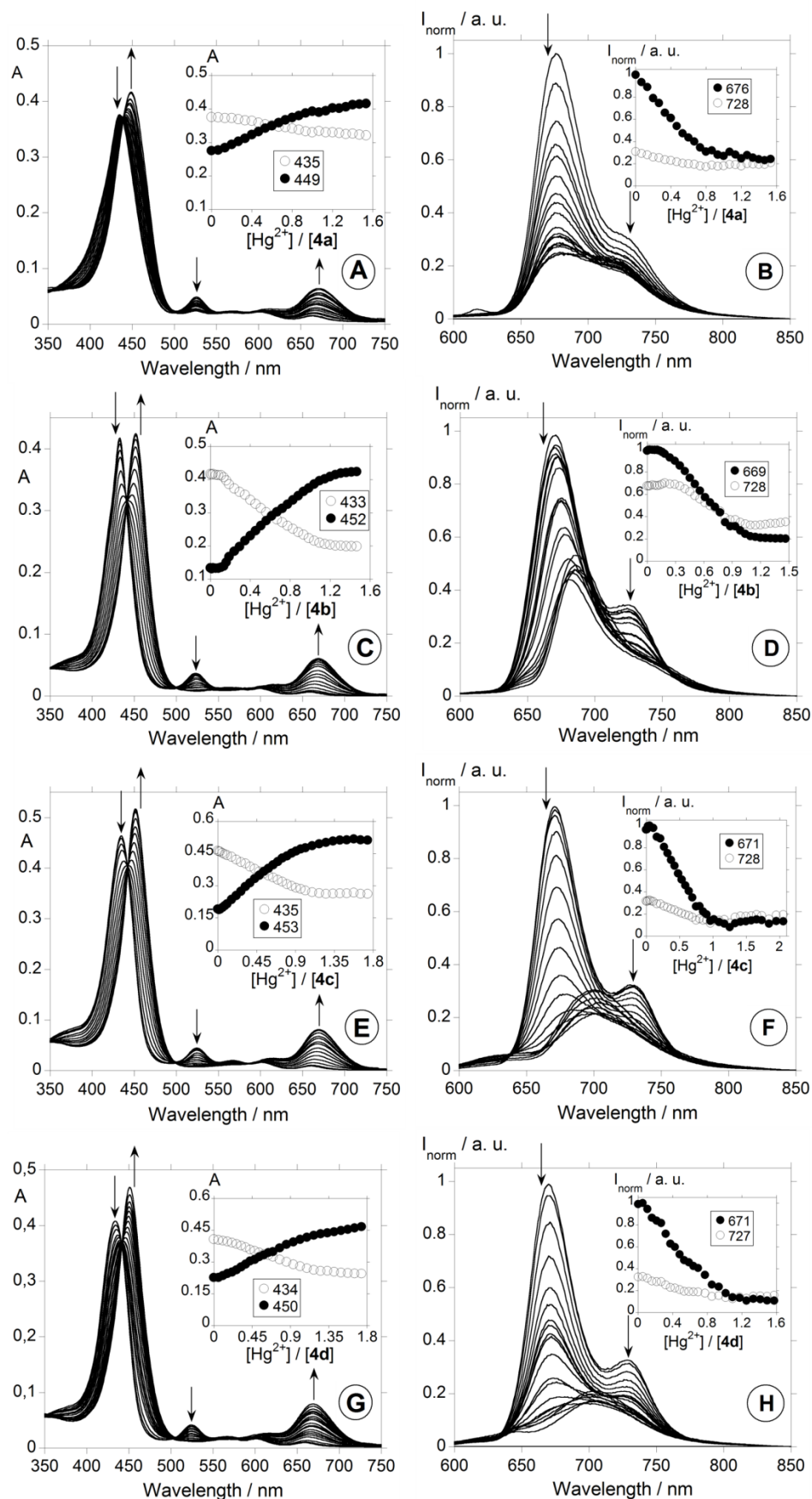


Figure 26_SM – Spectrophotometric (A, C, E and G) and spectrofluorimetric (B, D, F and H) titrations of compounds **4a, **4b**, **4c** and **4d** in chloroform as a function of added Hg^{2+} in acetonitrile. The insets show the absorption at 435 and 449 nm (A), 433 and 452 nm (C), 435 and 453 nm (E) and 434 and 450 nm (G); and the normalized fluorescence intensity at 676 and 728 nm (B), 669 and 728 nm (D), 671 and 728 nm (F) and 671 and 727 nm (H) ($[4a] = [4b] = [4c] = [4e] = 2.50 \times 10^{-6} M$; $\lambda_{exc4a} = 548$ nm, $\lambda_{exc4b} = 542$ nm, $\lambda_{exc4c} = 545$ nm, $\lambda_{exc4d} = 549$ nm).**

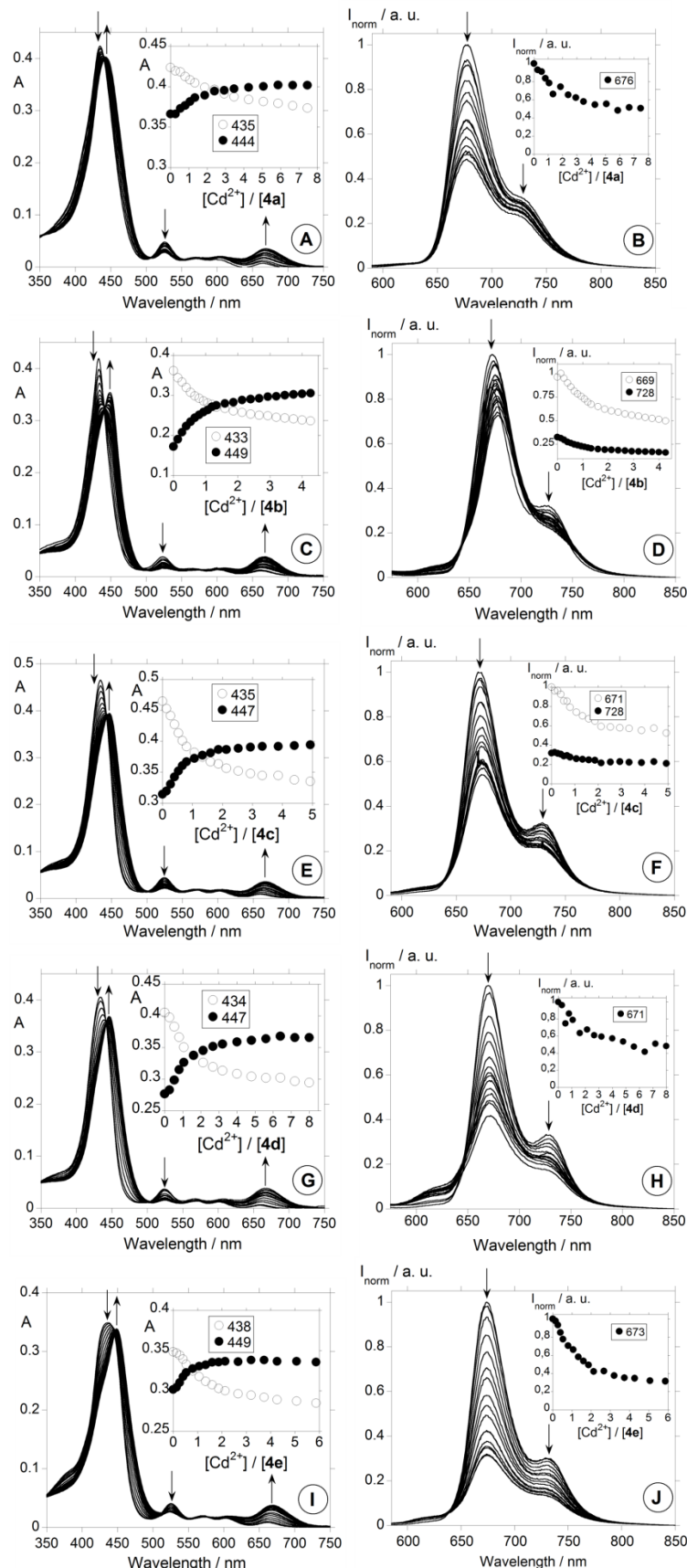


Figure 27_SM - Spectrophotometric (A, C, E, G and I) and spectrofluorimetric (B, D, F, H and J) titrations of compounds **4a, **4b**, **4c**, **4d** and **4e** in chloroform as a function of added Cd^{2+} in acetonitrile. The insets show the absorption at 435 and 444 nm (A), 433 and 449 nm (C), 435 and 447 nm (E) 434 and 447 nm (G) and 438 and 479 nm (I); and the normalized fluorescence intensity at 676 nm (B), 669 and 728 nm (D), 671 and 728 nm (F), 671 (H) and 673 nm (J) ($[4\mathbf{a}] = [4\mathbf{b}] = [4\mathbf{c}] = [4\mathbf{e}] = 2.50 \times 10^{-6} \text{ M}$; $\lambda_{\text{exc}4\mathbf{a}} = 548 \text{ nm}$, $\lambda_{\text{exc}4\mathbf{b}} = 542 \text{ nm}$, $\lambda_{\text{exc}4\mathbf{c}} = 545 \text{ nm}$, $\lambda_{\text{exc}4\mathbf{d}} = 549 \text{ nm}$, $\lambda_{\text{exc}4\mathbf{e}} = 545 \text{ nm}$).**

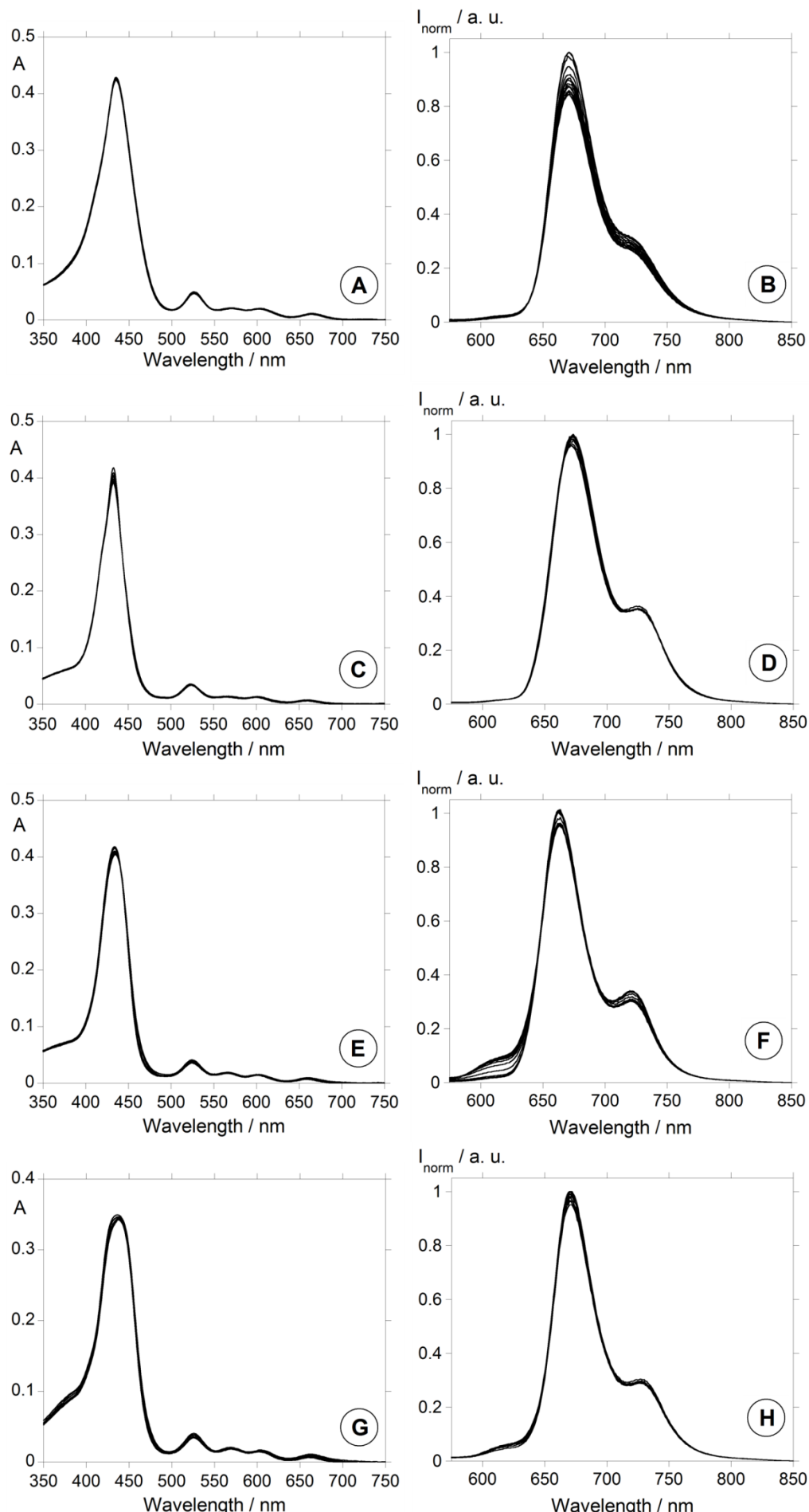


Figure 28_SM – Spectrophotometric (A, C, E and G) and spectrofluorimetric (B, D, F and H) titrations of compounds **4a**, **4b**, **4d** and **4e** in chloroform as a function of added Ag^+ in acetonitrile ($[\mathbf{4a}] = [\mathbf{4b}] = [\mathbf{4d}] = [\mathbf{4e}] = 2.50 \times 10^{-6} \text{ M}$; $\lambda_{\text{exc4a}} = 548 \text{ nm}$, $\lambda_{\text{exc4b}} = 542 \text{ nm}$, $\lambda_{\text{exc4d}} = 549 \text{ nm}$, $\lambda_{\text{exc4e}} = 545 \text{ nm}$).

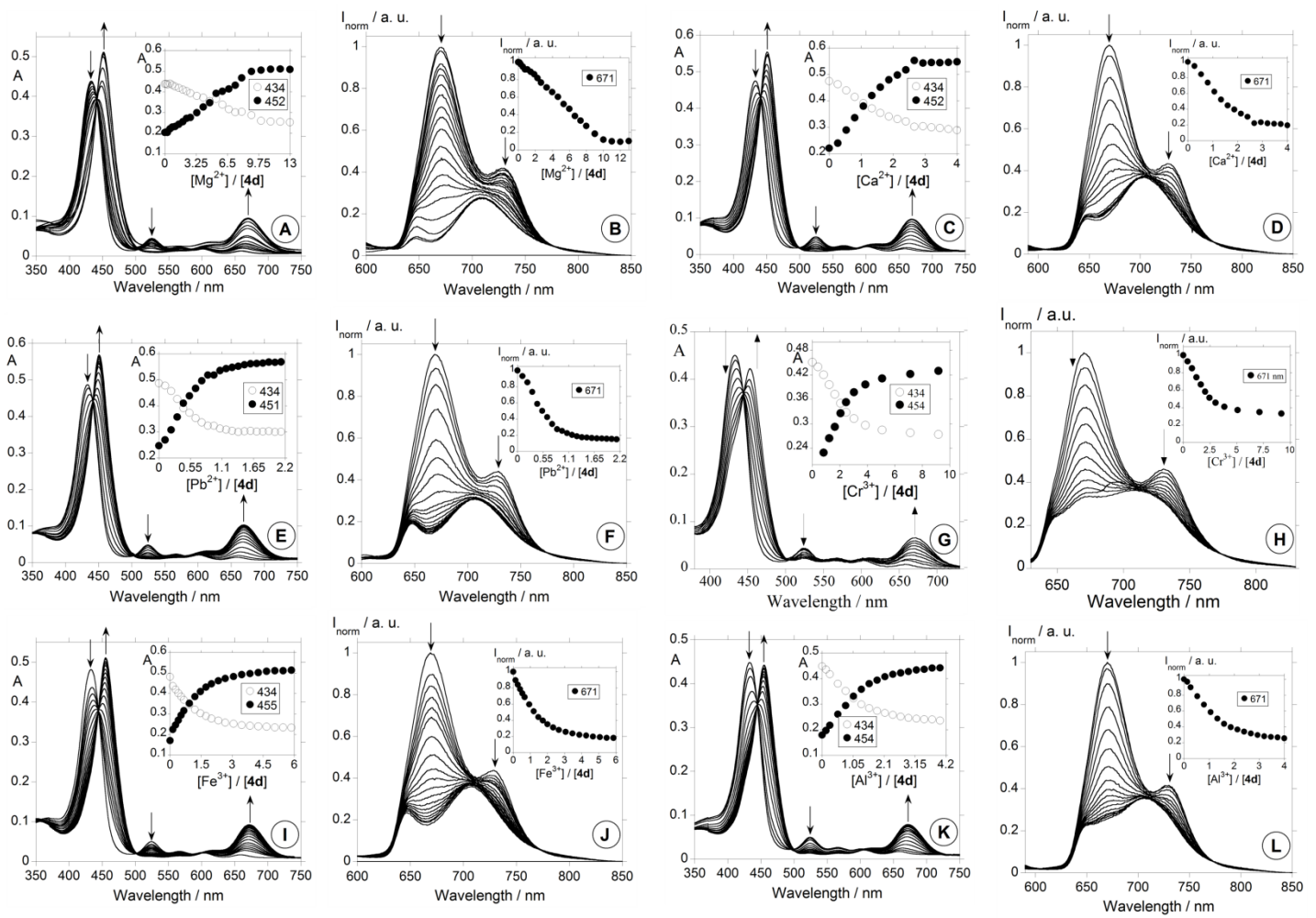


Figure 29_SM - Spectrophotometric (A, C, E, G, I and K) and spectrofluorimetric (B, D, F, H, J and L) titrations of compound **4d in chloroform as a function of added Mg^{2+} (A and B), Ca^{2+} (C and D), Pb^{2+} (E and F), Cr^{3+} (G and H), Fe^{3+} (I and J) and Al^{3+} (K and L) in acetonitrile. The insets show the absorption at 434 and 452 nm (A and C), 434 and 451 nm (E), 434 and 454 nm (G and K) and 434 and 455 nm (I); and the normalized fluorescence intensity at 671 nm (B, D, F, H, J and L) ($[4d] = 2.50 \times 10^{-6} M$, $\lambda_{exc4d} = 549$ nm; $[Mg^{2+}] = [Ca^{2+}] = [Cr^{3+}] = [Fe^{3+}] = [Al^{3+}] = 1.00 \times 10^{-3} M$; $[Pb^{2+}] = 4.70 \times 10^{-3} M$). (G and H)**

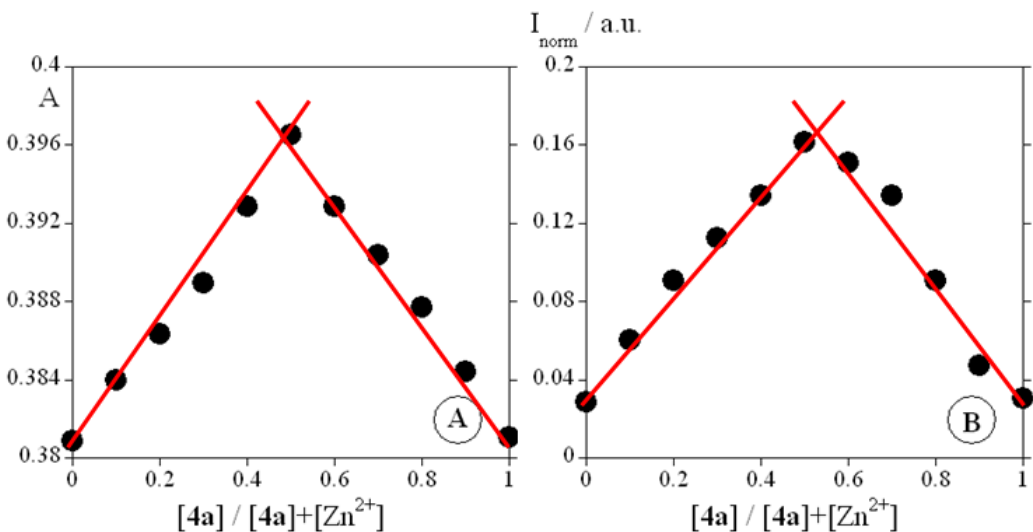


Figure 30_SM - Job's plot for the UV-Vis (**A**) and fluorescence emission (**B**) titration profiles of compound **4a** (2.50x10⁻⁶ M) with Zn²⁺ shows 1:1 (**4a**:Zn²⁺) complex stoichiometry: (**A**) with respect to 433 nm and (**B**) with respect to 634 nm.

Table 1_SM - Stability constants for chemosensor **4d** in the presence of Zn(NO₃)₂.xH₂O, Zn(OTf)₂.xH₂O Mg(OTf)₂.xH₂O, Pb(OTf)₂.xH₂O, Ca(BF₄)₂, Cr(NO₃)₃.xH₂O, Fe(NO₃)₃ and Al(NO₃)₃ in CHCl₃ for an interaction 1:1 (metal:ligand).

Compound	Interaction (M:L)	$\Sigma \log \beta$ (Abs)	$\Sigma \log \beta$ (Emiss)
4d	Zn(NO ₃) ₂ .xH ₂ O	6.58 ± 1.07x10 ⁻³	6.54 ± 9.77x10 ⁻²
	Zn(OTf) ₂ .xH ₂ O	6.85 ± 2.07x10 ⁻³	6.81 ± 1.92x10 ⁻²
	Mg(OTf) ₂ .xH ₂ O	4.33 ± 3.45x10 ⁻³	2.78 ± 1.47x10 ⁻²
	Ca(BF ₄) ₂	5.75 ± 2.21x10 ⁻³	5.74 ± 8.70x10 ⁻³
	Pb(OTf) ₂ .xH ₂ O	7.45 ± 3.11x10 ⁻³	7.54 ± 1.30x10 ⁻²
	Cr(NO ₃) ₃ .xH ₂ O	5.33 ± 1.31x10 ⁻³	5.39 ± 5.39x10 ⁻²
	Fe(NO ₃) ₃	5.83 ± 2.35x10 ⁻³	5.80 ± 8.35x10 ⁻³
	Al(NO ₃) ₃	5.94 ± 1.84x10 ⁻³	5.86 ± 2.19x10 ⁻²

Table 2_SM - Limits of detection (LOD) and quantification (LOQ) in ppb for Zn²⁺, Cu²⁺, Hg²⁺, Cd²⁺ and Ag⁺ with compounds **4a-e**.

Compound	Metal ion	LOD	LOQ
4a	Zn ²⁺	160 ± 10	240 ± 10
	Cu ²⁺	150 ± 10	950 ± 10
	Hg ²⁺	60 ± 10	260 ± 10
	Cd ²⁺	270 ± 10	1090 ± 10
4b	Zn ²⁺	80 ± 10	240 ± 10
	Cu ²⁺	70 ± 10	270 ± 10
	Hg ²⁺	230 ± 10	430 ± 10
	Cd ²⁺	270 ± 10	550 ± 10
4c	Zn ²⁺	160 ± 10	240 ± 10
	Cu ²⁺	70 ± 10	150 ± 10
	Hg ²⁺	190 ± 10	330 ± 10
	Cd ²⁺	180 ± 10	410 ± 10
	Ag ⁺	380 ± 10	780 ± 10
4d	Zn ²⁺	240 ± 10	560 ± 10
	Cu ²⁺	70 ± 10	320 ± 10
	Hg ²⁺	130 ± 10	190 ± 10
	Cd ²⁺	550 ± 10	1090 ± 10
4e	Zn ²⁺	160 ± 10	320 ± 10
	Cu ²⁺	70 ± 10	150 ± 10
	Hg ²⁺	330 ± 10	410 ± 10
	Cd ²⁺	140 ± 10	270 ± 10

IV - NMR titrations

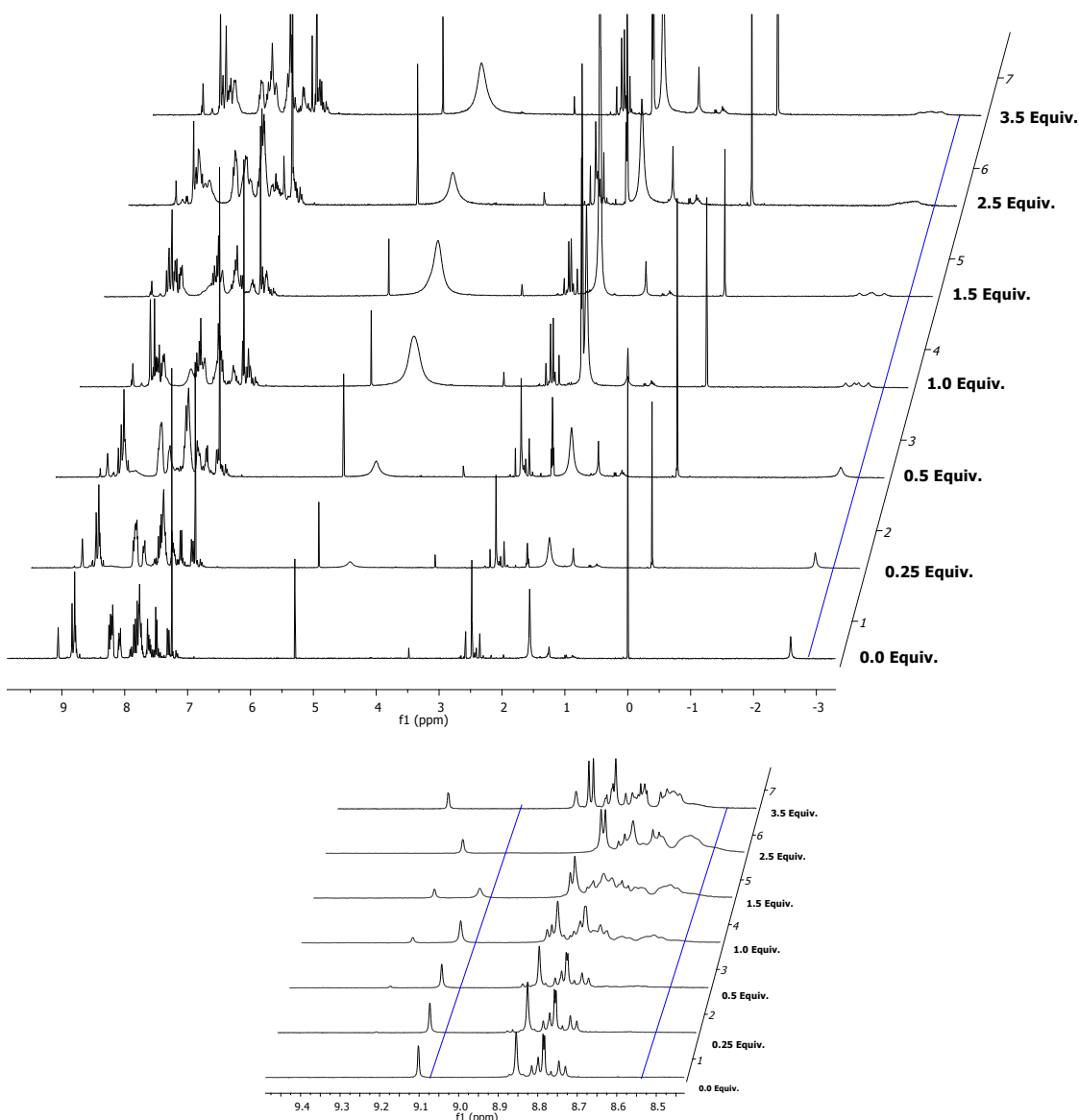


Figure 30_SM - ¹H NMR spectra of **4c** (2.5×10^{-3} mM) in CDCl₃ upon addition of increasing amounts of Zn²⁺ (from 0 to 3.5 equiv) in CD₃CN.

V - MALDI-TOF-MS titrations data

Table 3_SM - Major peaks observed in the metal titration of chemosensor **4b** followed by MALDI-TOF-MS.

Metal	Stoichiometry (ligand:metal)	Dried-droplet		Layer-by-Layer	
		<i>m/z</i>	Relative intensity (%)	<i>m/z</i>	Relative intensity (%)
Zn^{2+}	1:1	745.13	100.00 $[4b+H]^+$	745.15	100.00 $[4b+H]^+$
		806.01	38.00 $[(4b-2H)+Zn]^{+•}$	806.05	16.00 $[(4b-2H)+Zn]^{+•}$
	1:2	745.20	100.00 $[4b+H]^+$	744.16	100.00 $[4b]^{+•}$
		806.10	91.00 $[(4b-2H)+Zn]^{+•}$	944.10	17.00 $[(4b-2H)+Hg]^{+•}$
Hg^{2+}	1:1	745.36	100.00 $[4b+H]^+$	744.16	100.00 $[4b]^{+•}$
	1:2	745.17	100.00 $[4b+H]^+$	944.10	17.00 $[(4b-2H)+Hg]^{+•}$
Cu^{2+}	1:1	805.05	100.00 $[(4b-2H)+Cu]^{+•}$	745.13	100.00 $[4b+H]^+$
	1:2	805.05	100.00 $[(4b-2H)+Cu]^{+•}$	805.07	79.00 $[(4b-2H)+Cu]^{+•}$
Cd^{2+}	1:1	745.18	100.00 $[4b+H]^+$	745.17	100.00 $[4b+H]^+$
	1:2	745.18	100.00 $[4b+H]^+$	854.06	5.00 $[(4b-4H)+Cd]^{+•}$
Ag^+	1:1	745.13	100.00 $[4b+H]^+$	745.15	41.00 $[4b+H]^+$
		851.01	86.00 $[(4b-H)+Ag]^{+•}$	850.96	100.00 $[(4b-H)+Ag]^{+•}$
	1:2	745.13	56.00 $[4b+H]^+$		
		851.01	100.00 $[(4b-H)+Ag]^{+•}$		

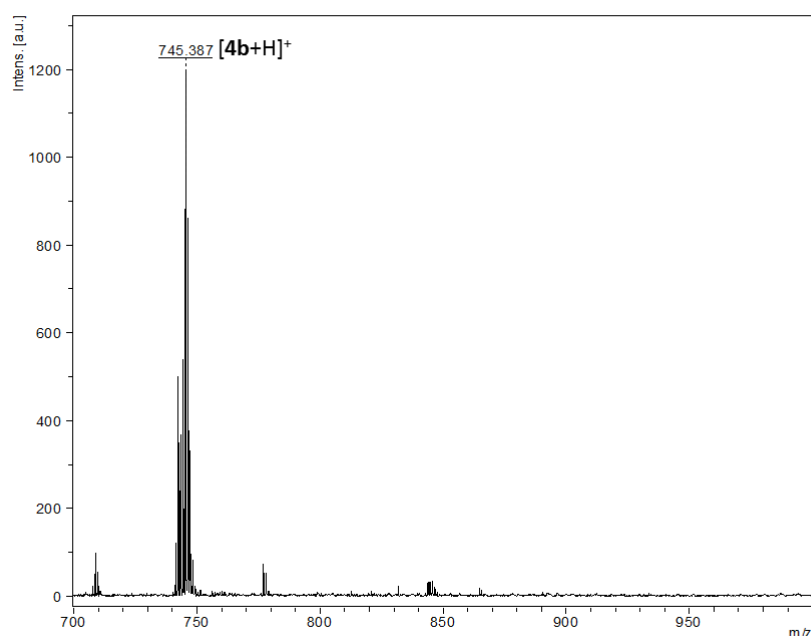


Figure 31_SM - MALDI-TOF mass spectra of compound **4b**.

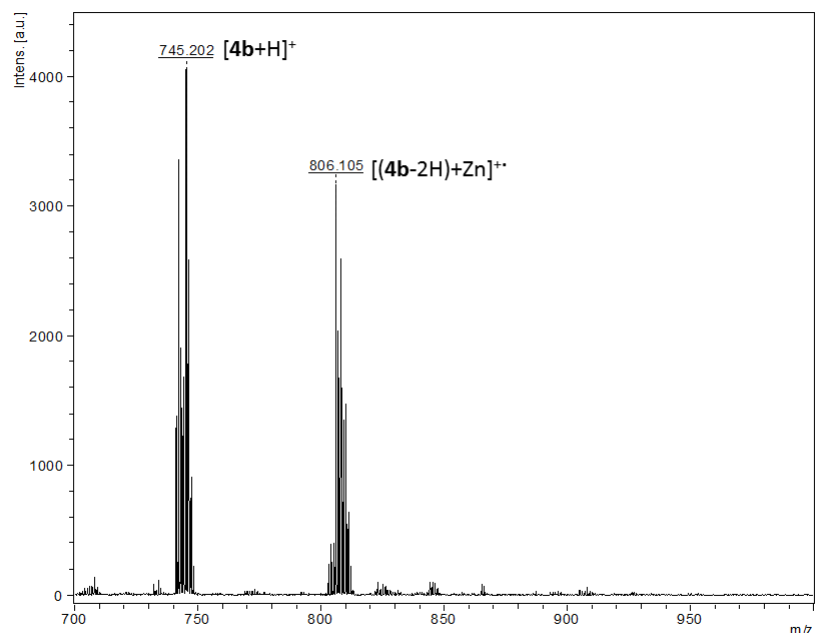
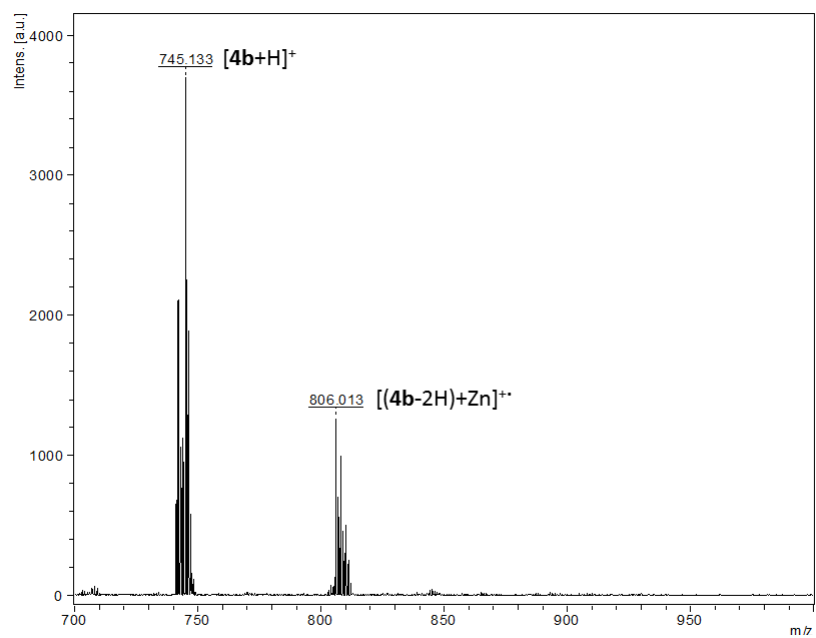


Figure 32_SM - MALDI-TOF mass spectra of compound **4b** after titration with 1 equiv. (above) and 2 equiv. of $\text{Zn}(\text{BF}_4)_2 \cdot x\text{H}_2\text{O}$ (below) (*dried-droplet method*).

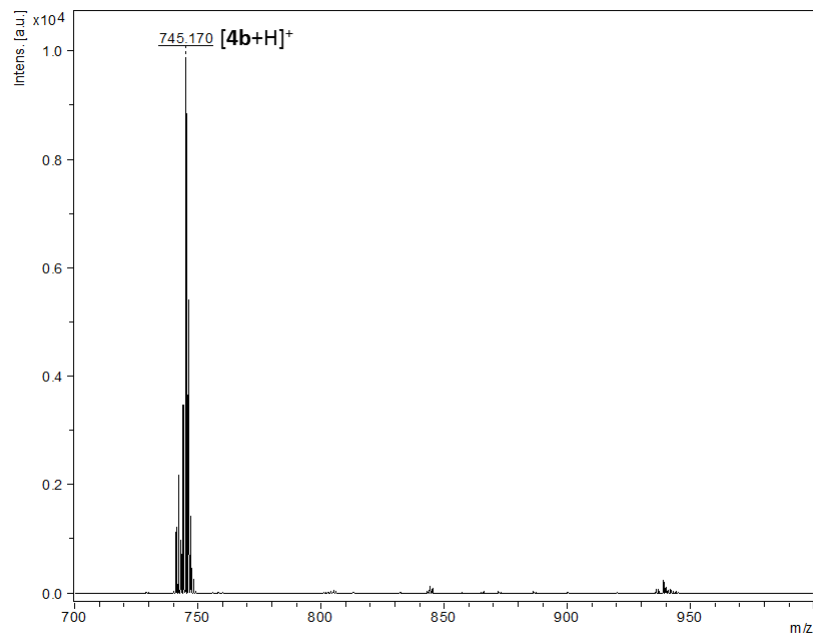
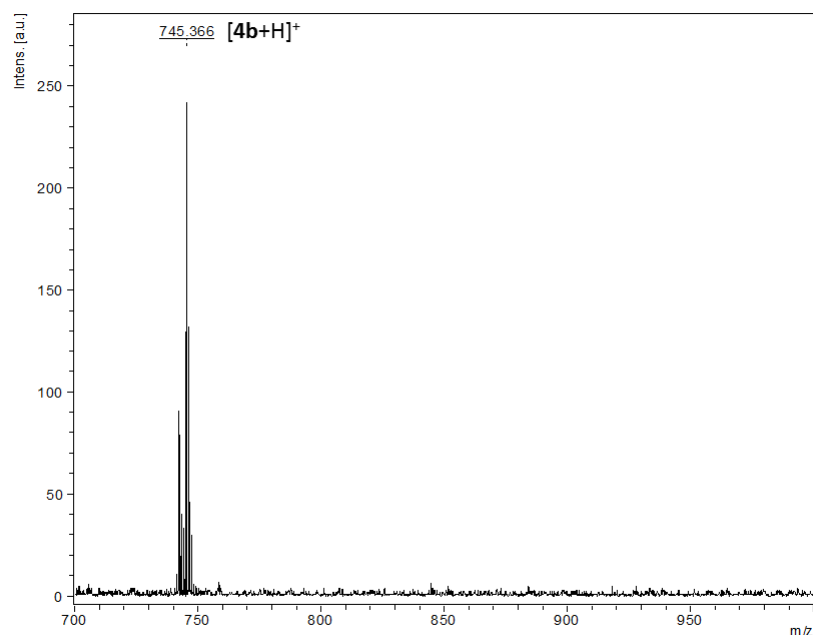


Figure 33_SM - MALDI-TOF mass spectra of compound **4b** after titration with 1 equiv. (above) and 2 equiv. of $Hg(BF_4)_2 \cdot xH_2O$ (below) (*dried-droplet method*).

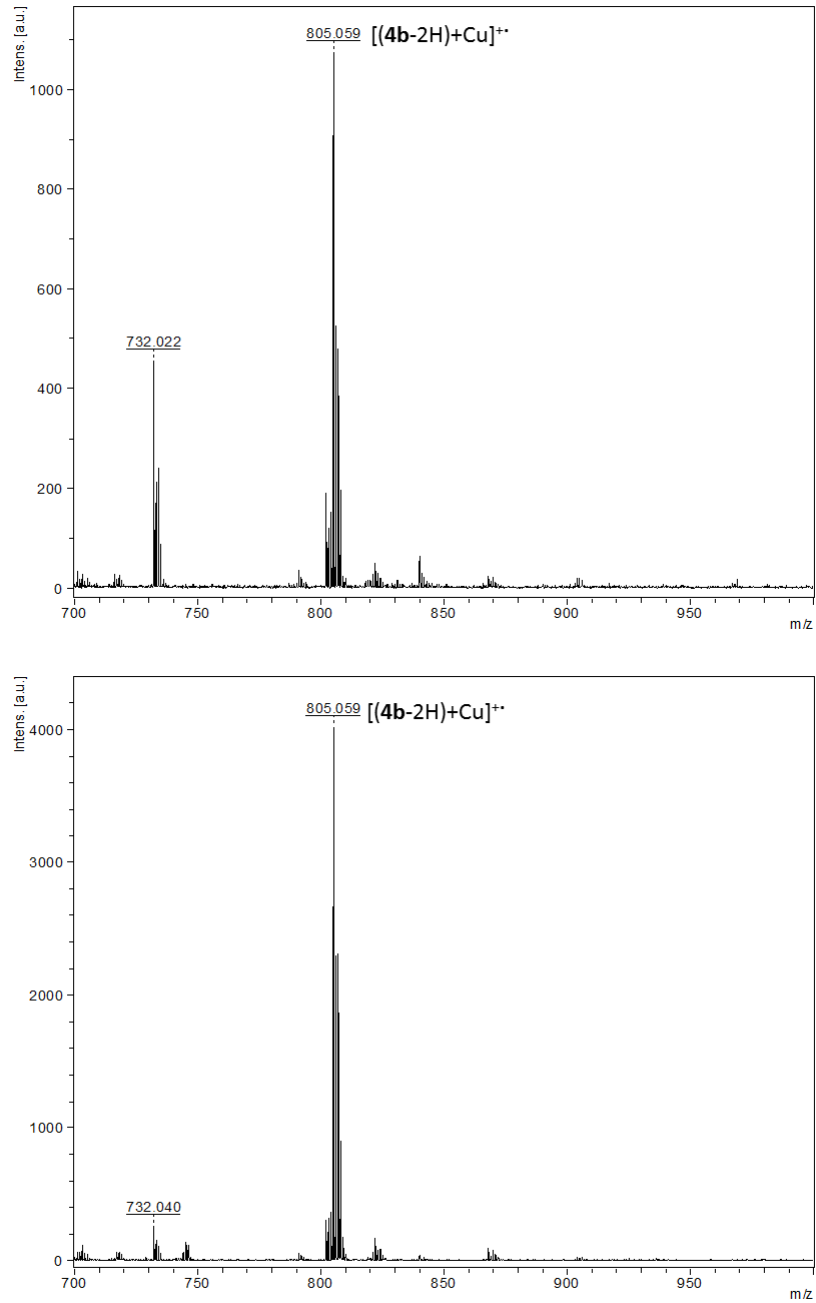


Figure 34_SM - MALDI-TOF mass spectra of compound **4b** after titration with 1 equiv. (above) and 2 equiv. of $\text{Cu}(\text{BF}_4)_2 \cdot x\text{H}_2\text{O}$ (below) (*dried-droplet method*).

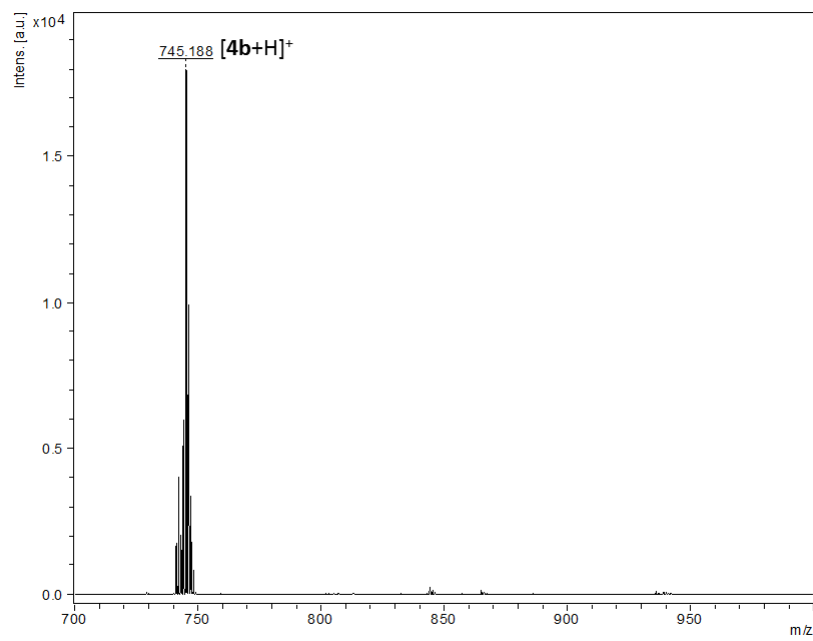
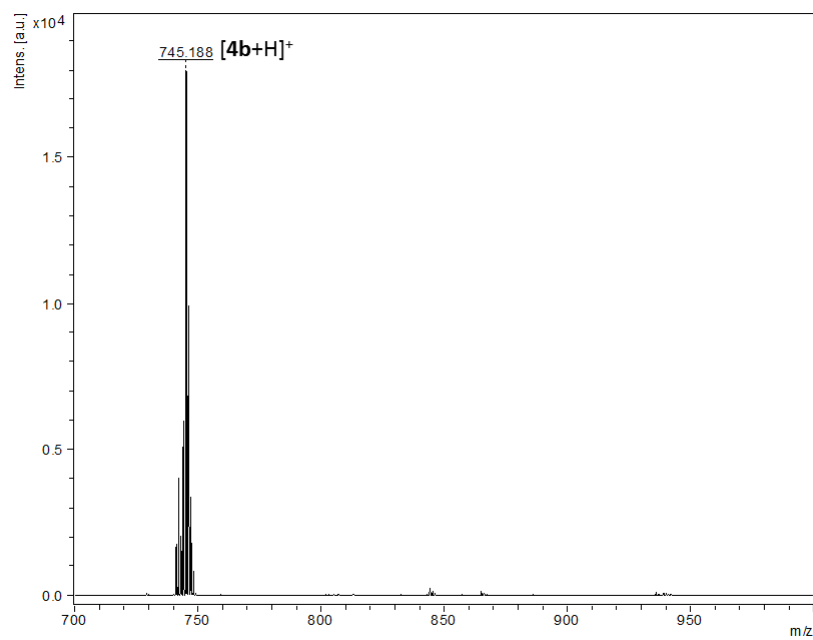


Figure 35_SM - MALDI-TOF mass spectra of compound **4b** after titration with 1 equiv. (above) and 2 equiv. of $\text{Cd}(\text{BF}_4)_2 \cdot x\text{H}_2\text{O}$ (below) (*dried-droplet method*).

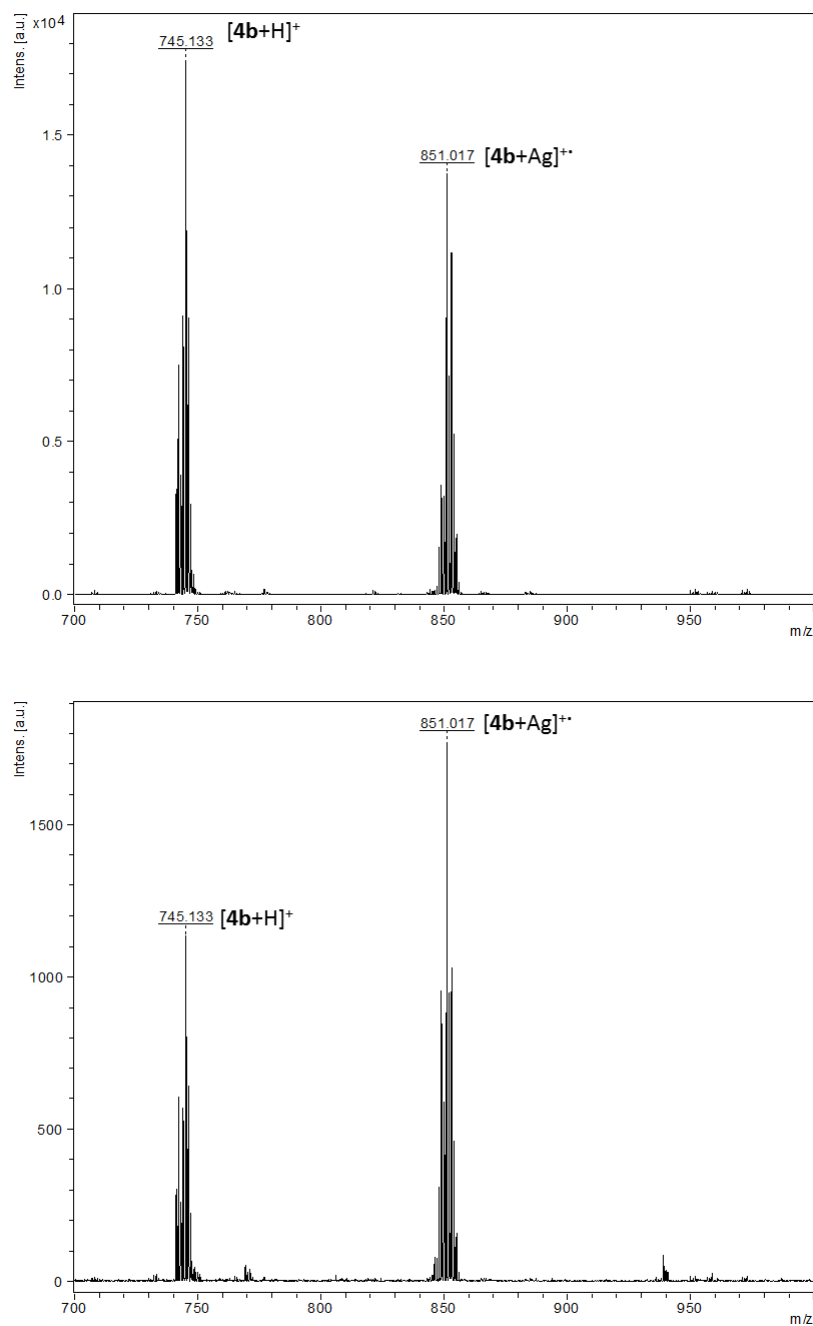


Figure 36_SM - MALDI-TOF mass spectra of compound **4b** after titration with 1 equiv. (above) and 2 equiv. of $\text{Ag}(\text{BF}_4)_x \cdot \text{H}_2\text{O}$ (below) (*dried-droplet method*).

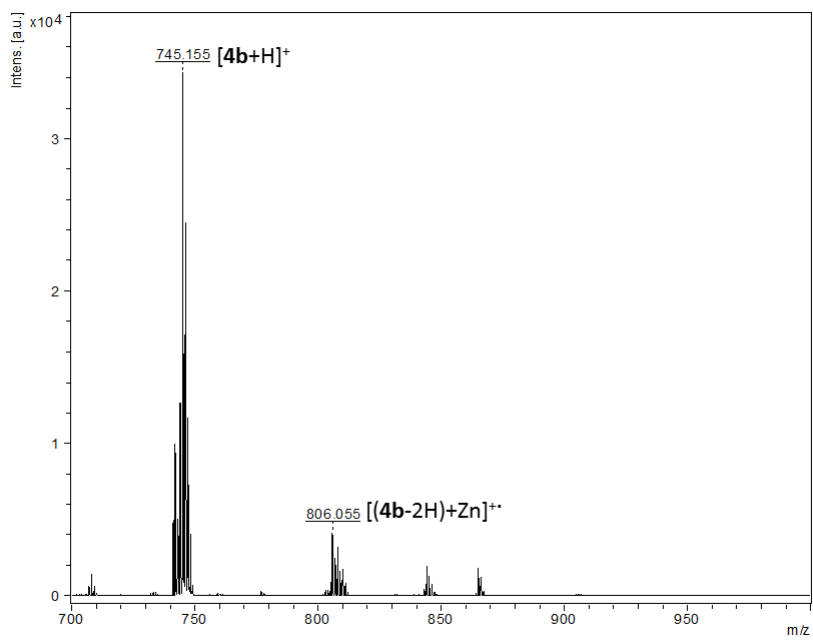


Figure 37_SM - MALDI-TOF mass spectra of compound **4b** after titration with of $Zn(BF_4)_2 \cdot xH_2O$ (*layer-by-layer method*).

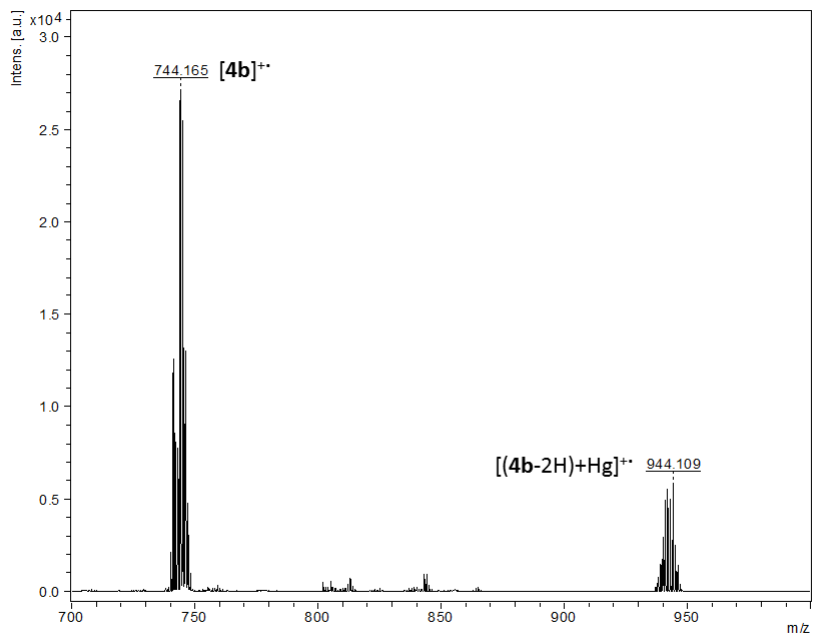


Figure 38_SM. MALDI-TOF mass spectra of compound **4b** after titration with of $Hg(BF_4)_2 \cdot xH_2O$ (*layer-by-layer method*).

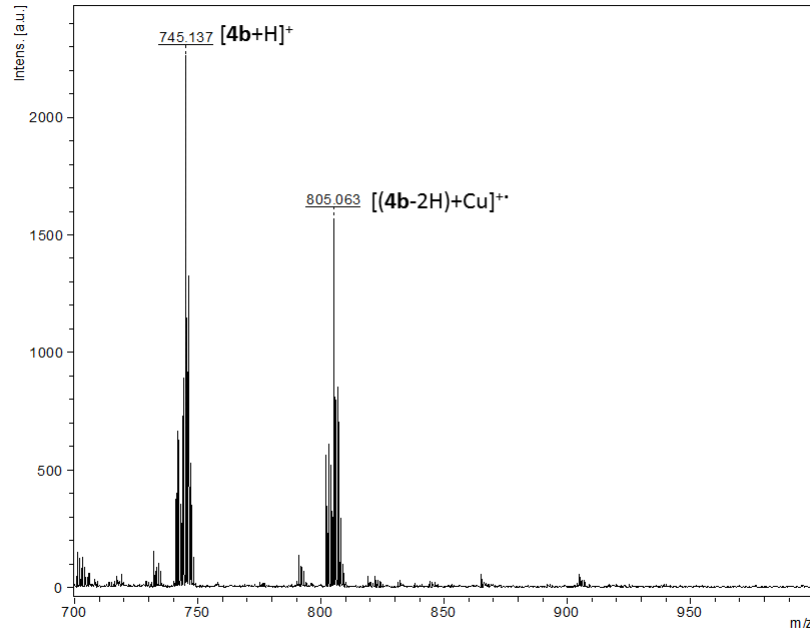


Figure 39_SM - MALDI-TOF mass spectra of compound **4b** after titration with of $\text{Cu}(\text{BF}_4)_2 \cdot x\text{H}_2\text{O}$ (*layer-by-layer method*).

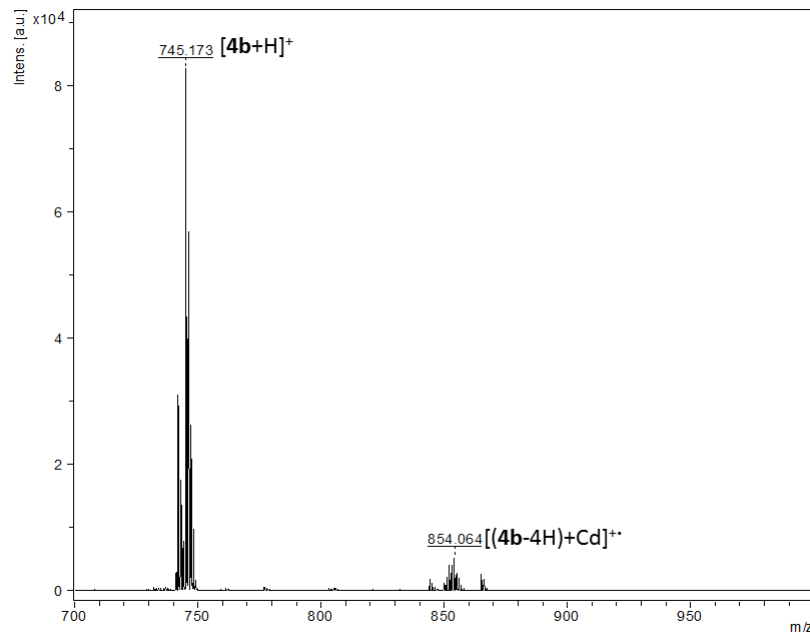


Figure 40_SM - MALDI-TOF mass spectra of compound **4b** after titration with of $\text{Cd}(\text{BF}_4)_2 \cdot x\text{H}_2\text{O}$ (*layer-by-layer method*).

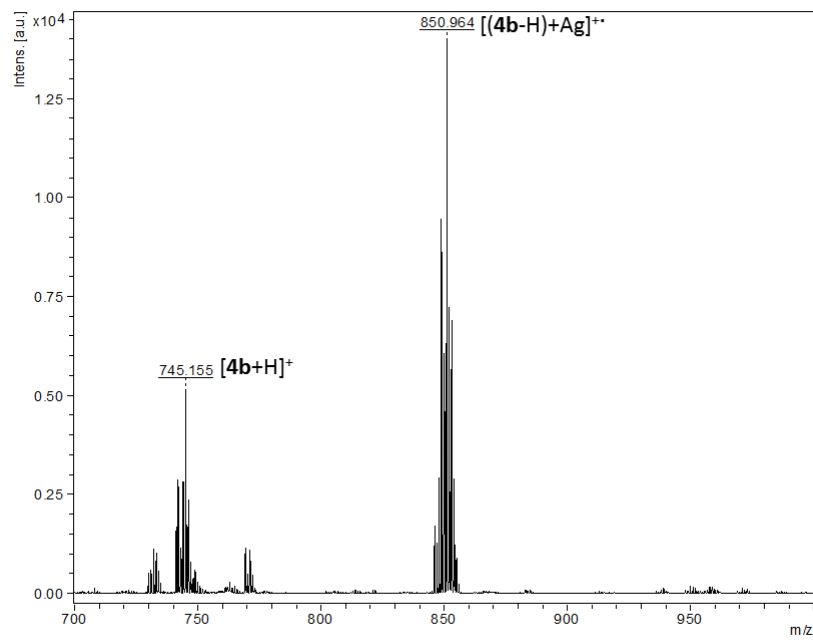


Figure 41_SM - MALDI-TOF mass spectra of compound **4b** after titration with of $\text{Ag}(\text{BF}_4)_x\text{H}_2\text{O}$ (*layer-by-layer method*).

Table 4_SM - Major peaks observed in the metal titration of chemosensor **4d** followed by MALDI-TOF-MS.

Metal	Stoichiometry (ligand:metal)	Dried-droplet		Layer-by-Layer	
		<i>m/z</i>	Relative intensity (%)	<i>m/z</i>	Relative intensity (%)
Zn ²⁺	1:1	775.17	100.00 [4d+H] ⁺	775.09	100.00 [4d+H] ⁺
		836.08	41.00 [(4d-2H)+Zn] ⁺		835.99 18.00 [(4d-3H)+Zn] ⁺
	1:2	775.10	100.00 [4d+H] ⁺	974.03	17.00 [(4d-2H)+Hg] ⁺
		835.96	96.00 [(4d-3H)+Zn] ⁺		
Hg ²⁺	1:1	775.26	100.00 [4d+H] ⁺	775.11	100.00 [4d+H] ⁺
	1:2	775.26	100.00 [4d+H] ⁺	835.09	54.00 [(4d-2H)+Cu] ⁺
Cu ²⁺	1:1	775.24	100.00 [4d+H] ⁺	775.09	100.00 [4d+H] ⁺
		835.17	21.00 [(4d-2H)+Cu] ⁺		
	1:2	835.09	100.00 [(4d-2H)+Cu] ⁺	835.02	54.00 [(4d-2H)+Cu] ⁺
		852.13	35.00 [(4d-3H)+Cu+H ₂ O] ⁺		
Cd ²⁺	1:1	775.28	100.00 [4d+H] ⁺	775.09	100.00 [4d+H] ⁺
		884.20	38.00 [(4d-4H)+Cd] ⁺		883.95 17.00 [(4d-5H)+Cd] ⁺
	1:2	775.28	100.00 [4d+H] ⁺	880.92	100.00 [(4d-H)+Ag] ⁺
		884.20	41.00 [(4d-4H)+Cd] ⁺		
Ag ⁺	1:1	775.19	100.00 [4d+H] ⁺	775.09	30.00 [4d+H] ⁺
		881.07	68.00 [4d+Ag] ⁺		
	1:2	775.17	82.00 [4d+H] ⁺	880.92	100.00 [(4d-H)+Ag] ⁺
		881.05	100.00 [4d+Ag] ⁺		

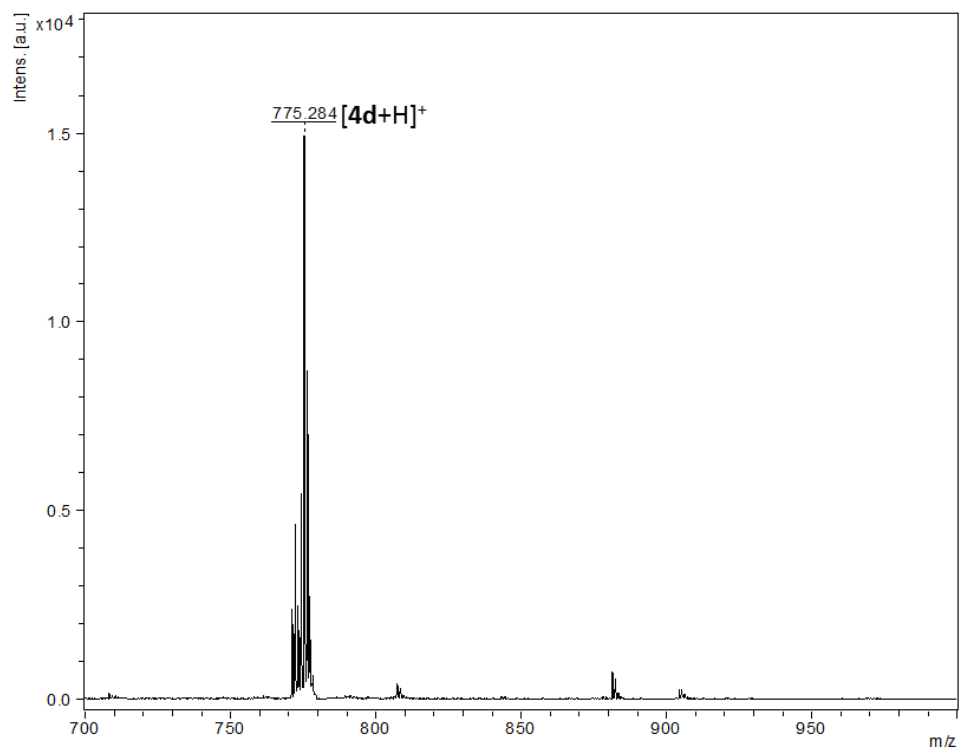


Figure 42_SM - MALDI-TOF mass spectra of compound **4d**.

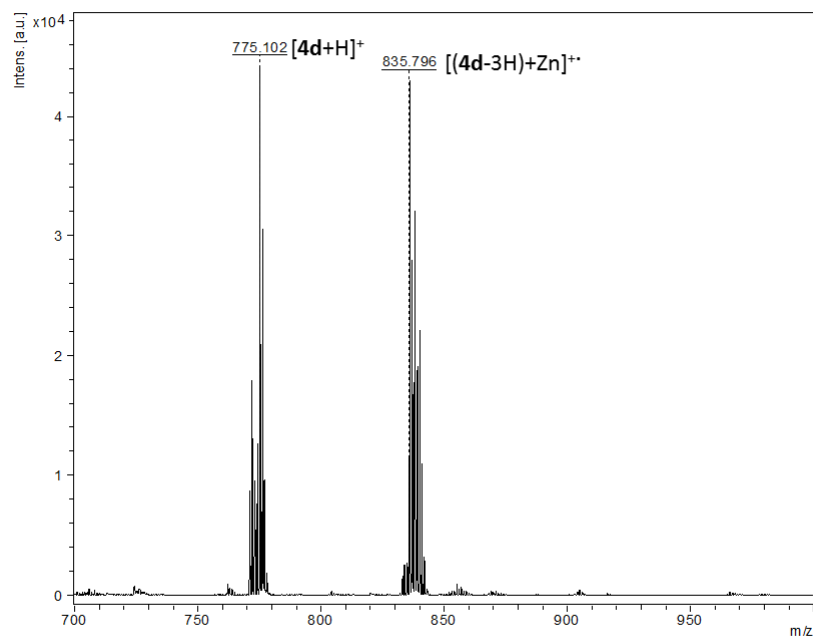
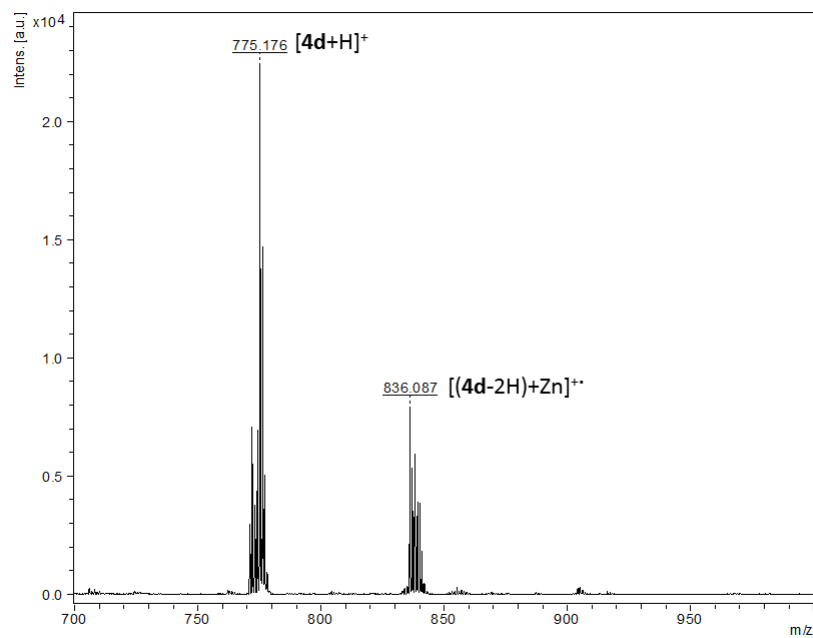


Figure 43_SM - MALDI-TOF mass spectra of compound **4d** after titration with 1 equiv. (above) and 2 equiv. of $\text{Zn}(\text{BF}_4)_2 \cdot x\text{H}_2\text{O}$ (below) (*dried-droplet method*).

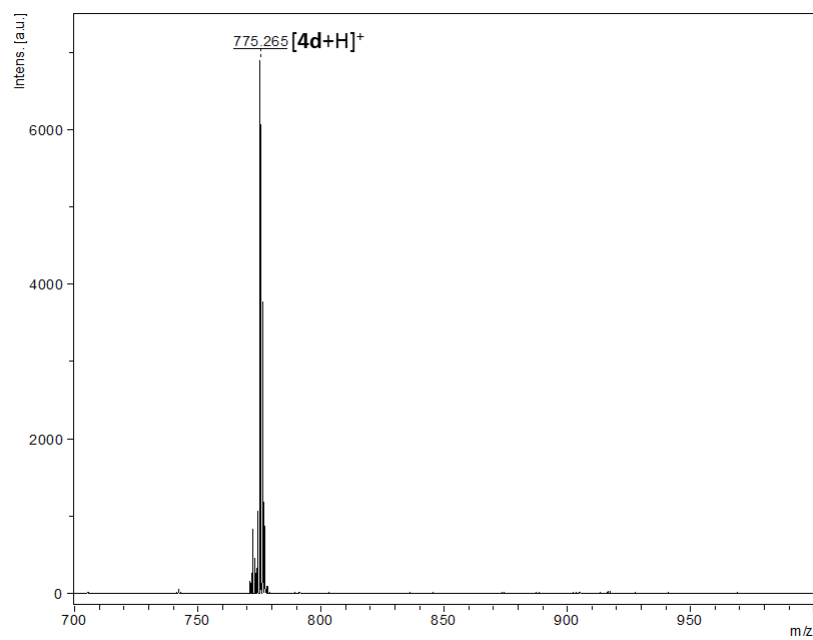


Figure 44_SM - MALDI-TOF mass spectra of compound **4d** after titration with 1 equiv. and 2 equiv. of $\text{Hg}(\text{BF}_4)_2 \cdot x\text{H}_2\text{O}$ (*dried-droplet method*).

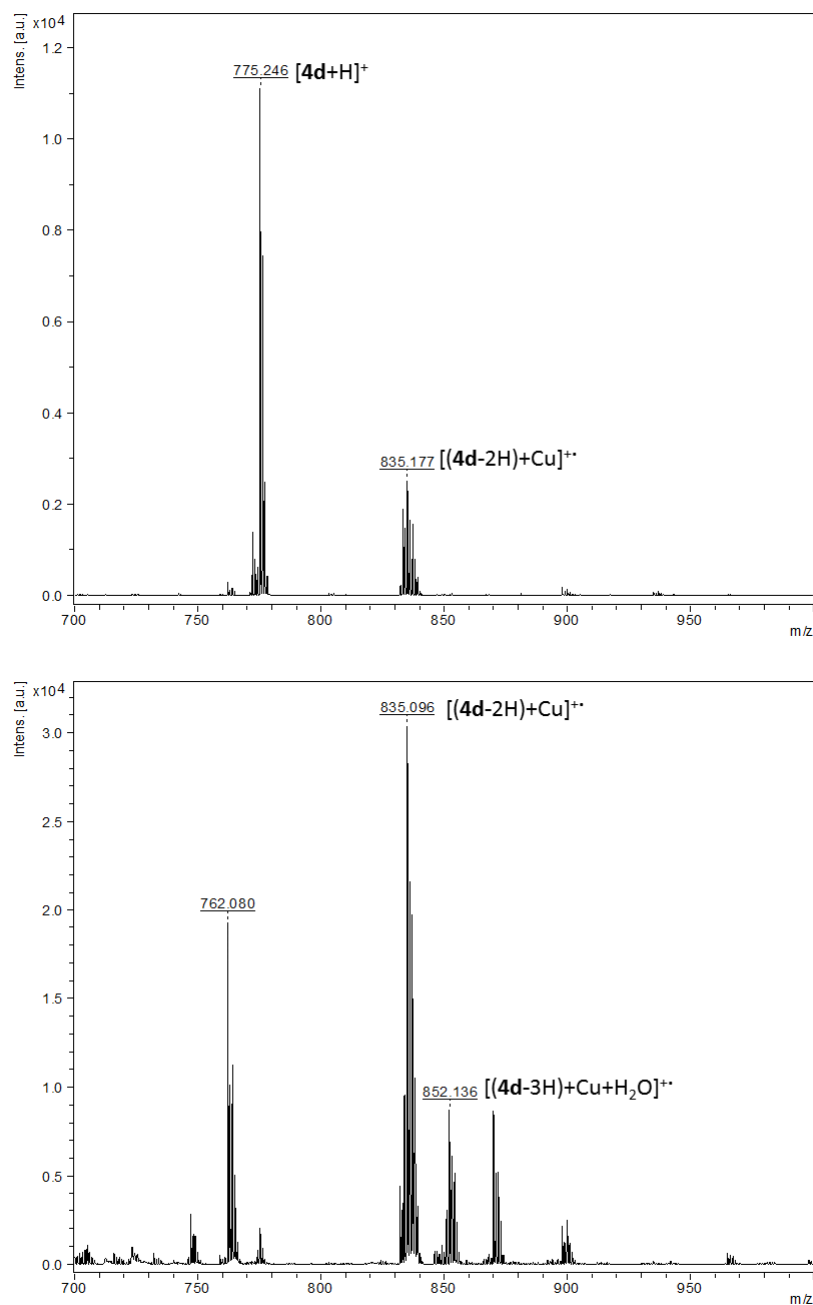


Figure 45_SM - MALDI-TOF mass spectra of compound **4d** after titration with 1 equiv. (above) and 2 equiv. of $Cu(BF_4)_2 \cdot xH_2O$ (below) (*dried-droplet method*).

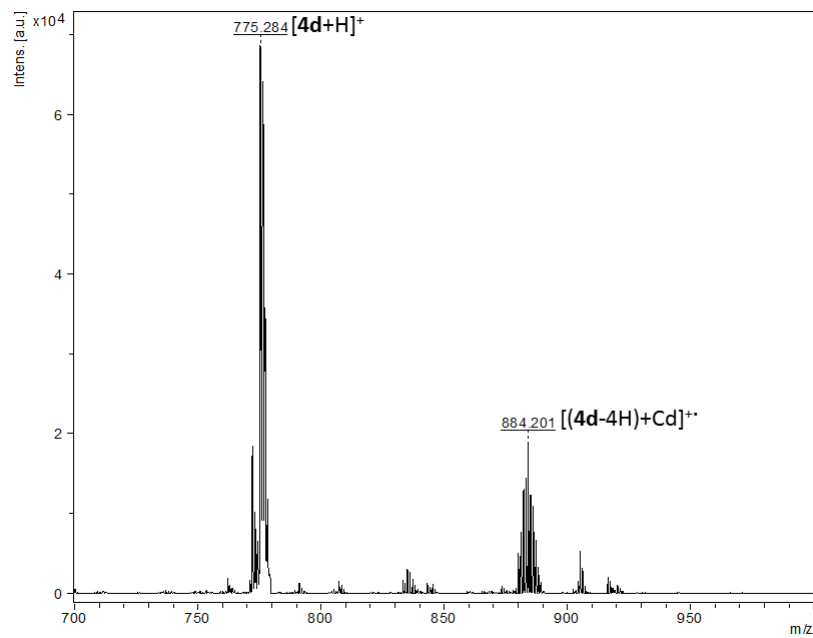
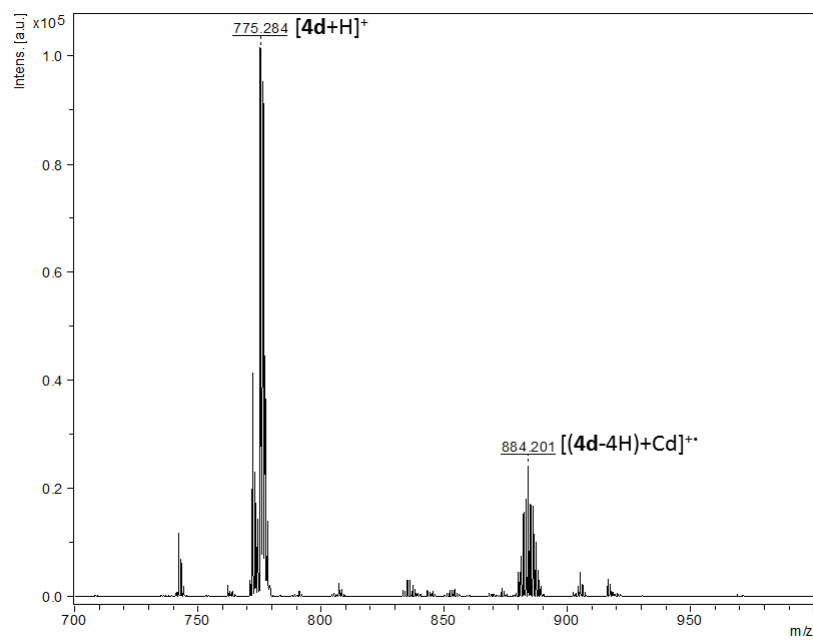


Figure 46_SM - MALDI-TOF mass spectra of compound **4d** after titration with 1 equiv. (above) and 2 equiv. of $\text{Cd}(\text{BF}_4)_2 \cdot x\text{H}_2\text{O}$ (below) (*dried-droplet method*).

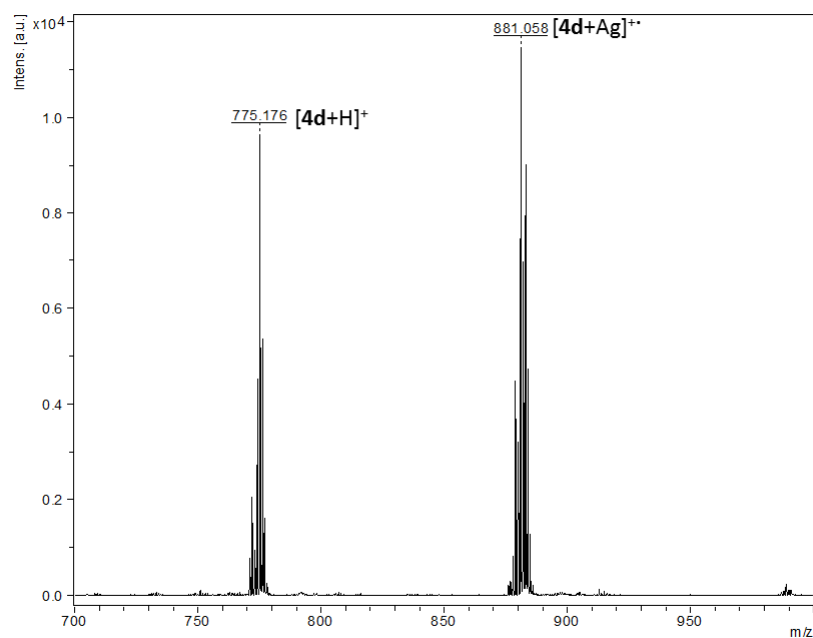
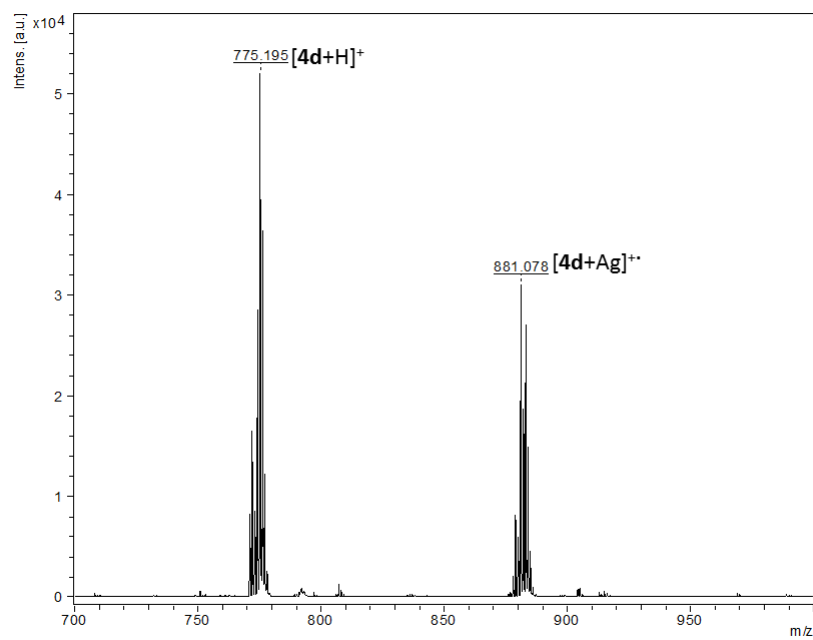


Figure 47_SM - MALDI-TOF mass spectra of compound **4d** after titration with 1 equiv. (above) and 2 equiv. of $\text{Ag}(\text{BF}_4)_x\text{H}_2\text{O}$ (below) (*dried-droplet method*).

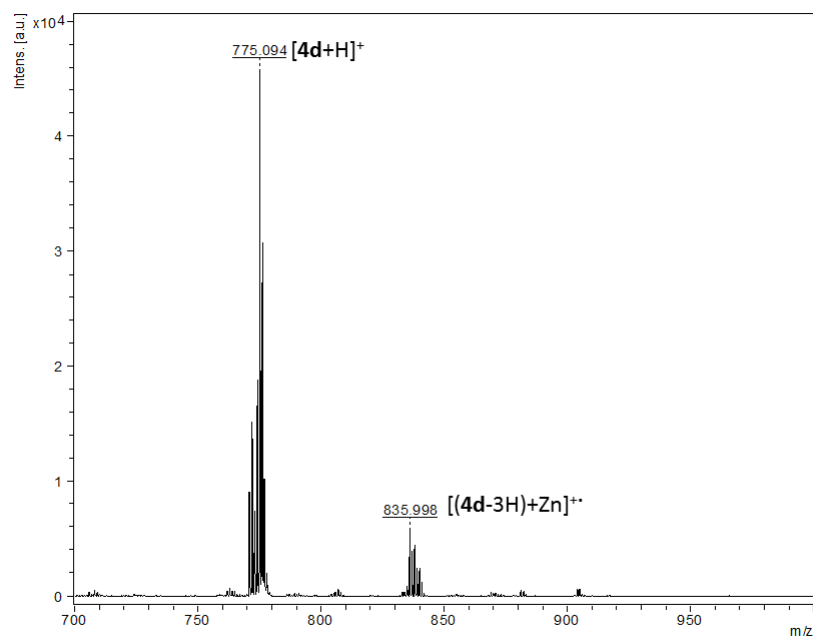


Figure 48_SM - MALDI-TOF mass spectra of compound **4d** after titration with of $\text{Zn}(\text{BF}_4)_2 \cdot x\text{H}_2\text{O}$ (*layer-by-layer method*).

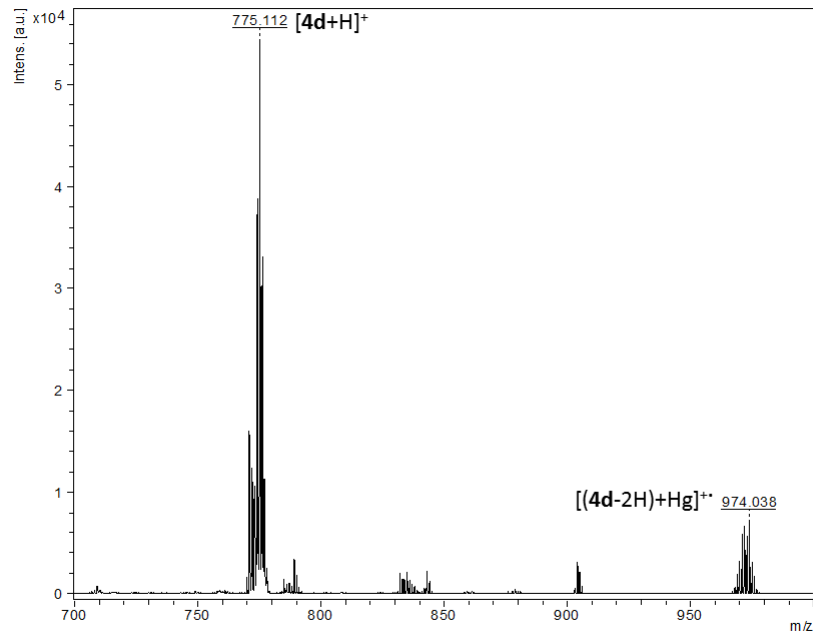


Figure 49_SM - MALDI-TOF mass spectra of compound **4d** after titration with of $\text{Hg}(\text{BF}_4)_2 \cdot x\text{H}_2\text{O}$ (*layer-by-layer method*).

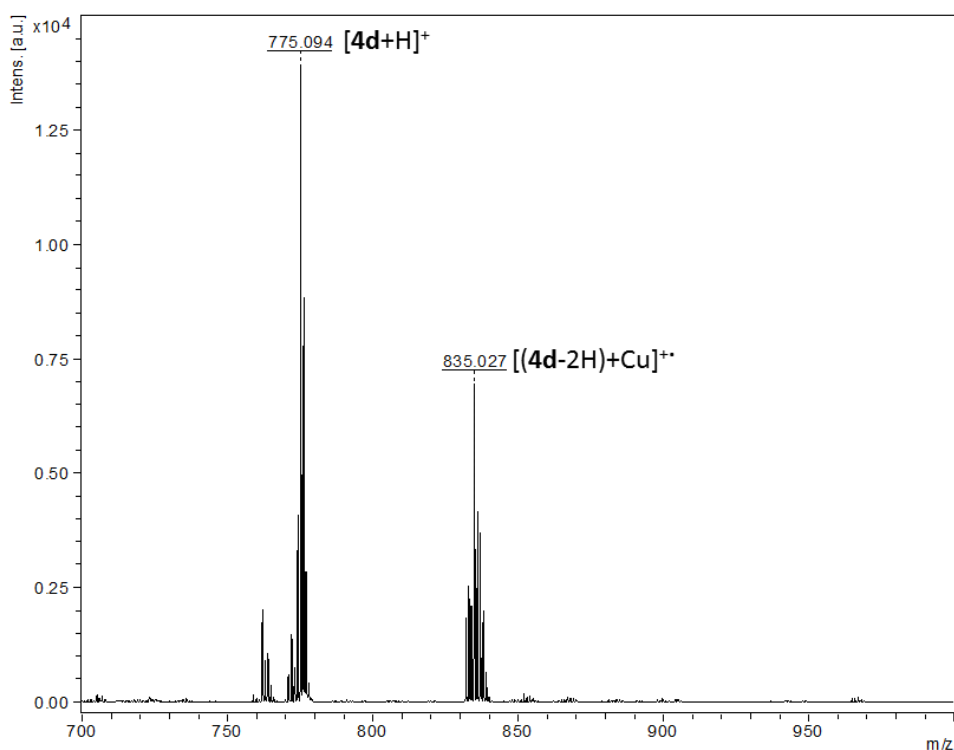


Figure 50_SM - MALDI-TOF mass spectra of compound **4d** after titration with of $\text{Cu}(\text{BF}_4)_2 \cdot x\text{H}_2\text{O}$ (*layer-by-layer method*).

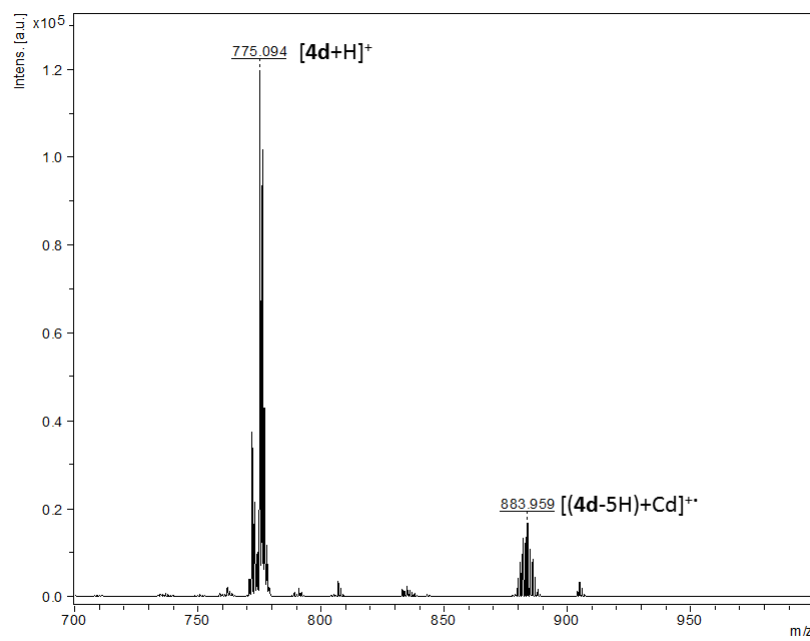


Figure 51_SM - MALDI-TOF mass spectra of compound **4d** after titration with of $\text{Cd}(\text{BF}_4)_2 \cdot x\text{H}_2\text{O}$ (*layer-by-layer method*).

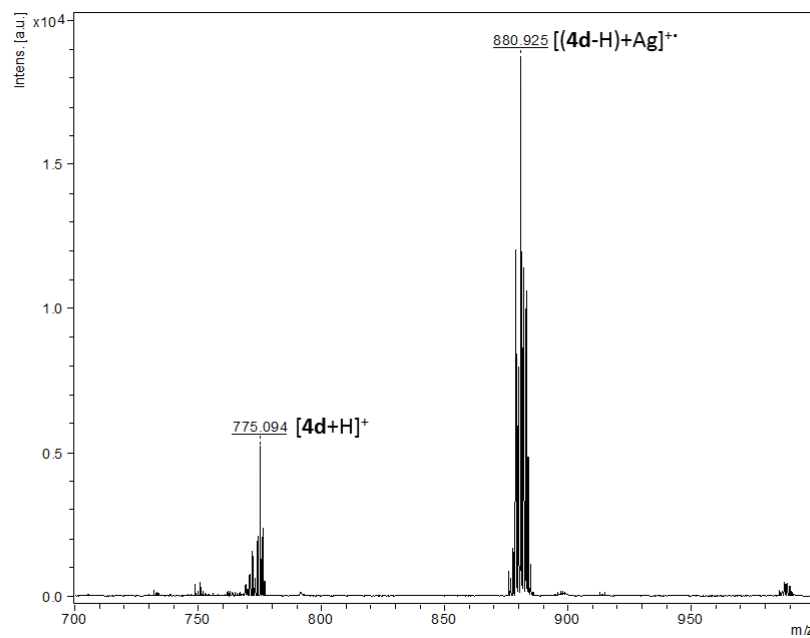


Figure 52_SM - MALDI-TOF mass spectra of compound **4d** after titration with of $\text{Ag}(\text{BF}_4)_2 \cdot x\text{H}_2\text{O}$ (*layer-by-layer method*).

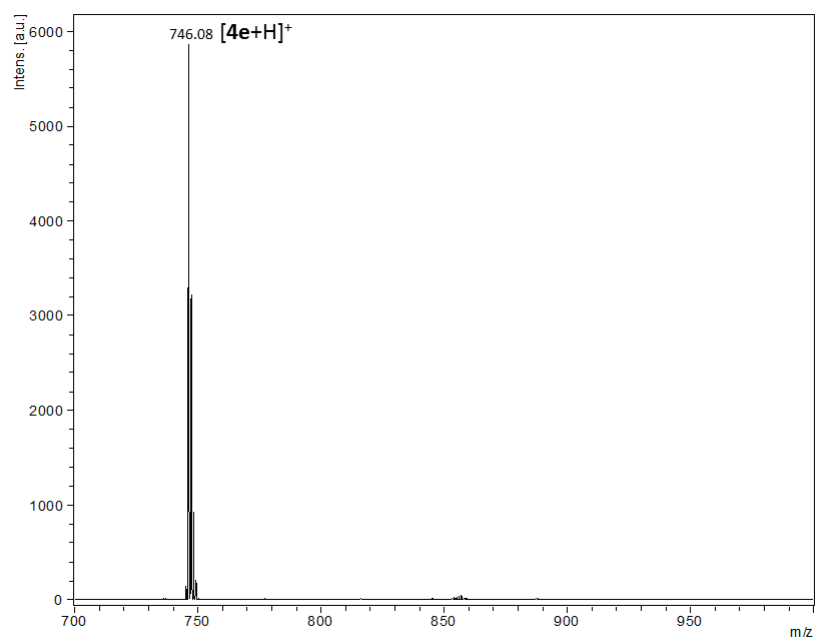


Figure 53_SM - MALDI-TOF mass spectra of compound **4e**.

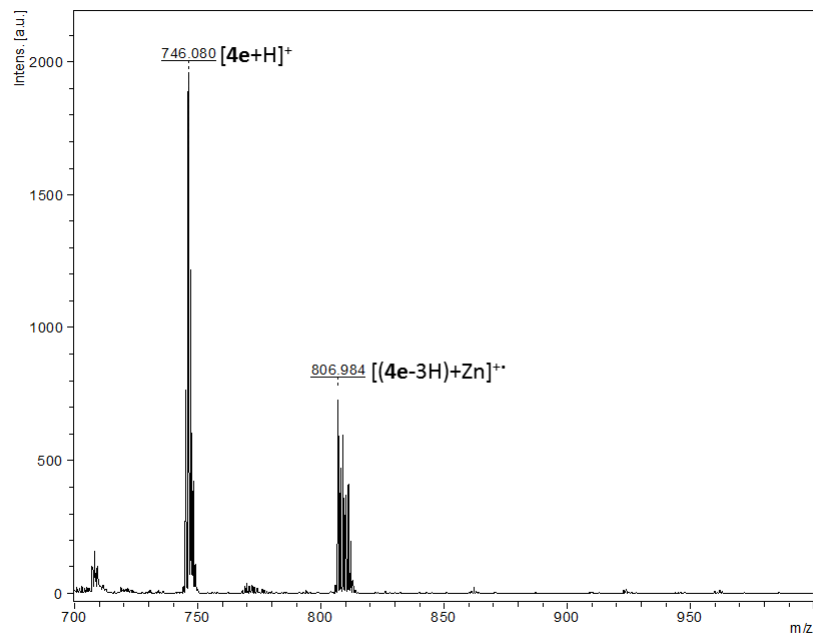


Figure 54_SM - MALDI-TOF mass spectra of compound **4e** after titration with 2 equiv. of $\text{Zn}(\text{BF}_4)_2 \cdot x\text{H}_2\text{O}$ (*dried-droplet method*).

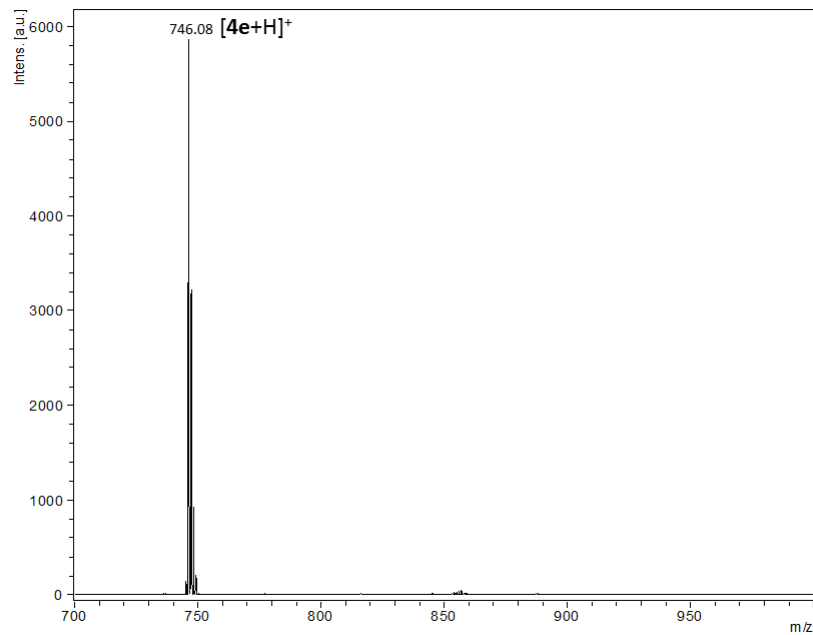


Figure 55_SM - MALDI-TOF mass spectra of compound **4e** after titration with 1 equiv. and 2 equiv. of $\text{Hg}(\text{BF}_4)_2 \cdot x\text{H}_2\text{O}$ (*dried-droplet method*).

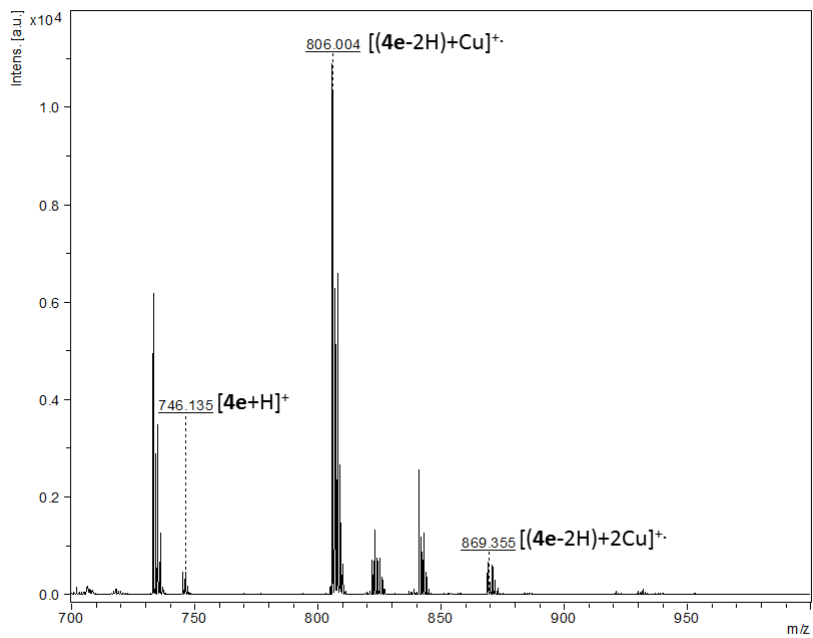
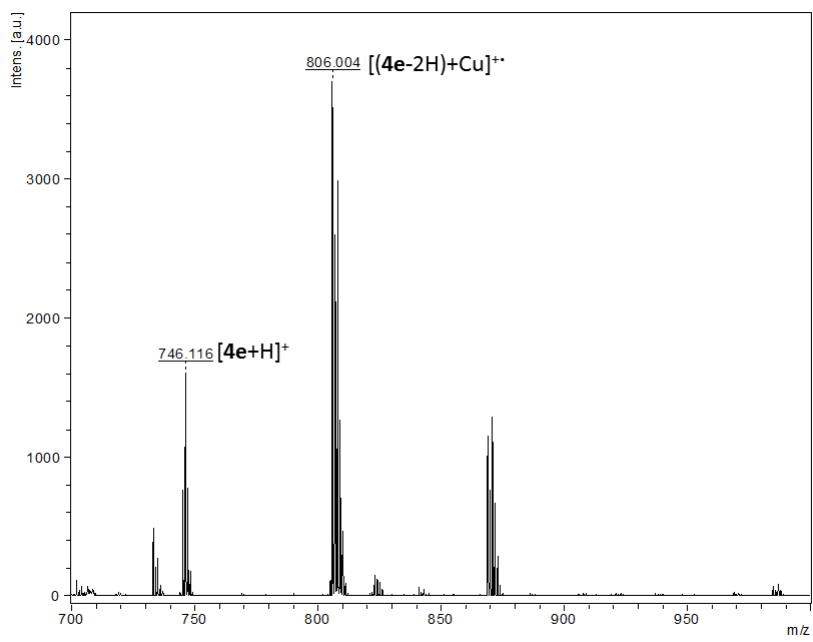


Figure 56_SM - MALDI-TOF mass spectra of compound **4e** after titration with 1 equiv. (above) and 2 equiv. of $\text{Cu}(\text{BF}_4)_2 \cdot x\text{H}_2\text{O}$ (below) (*dried-droplet method*).

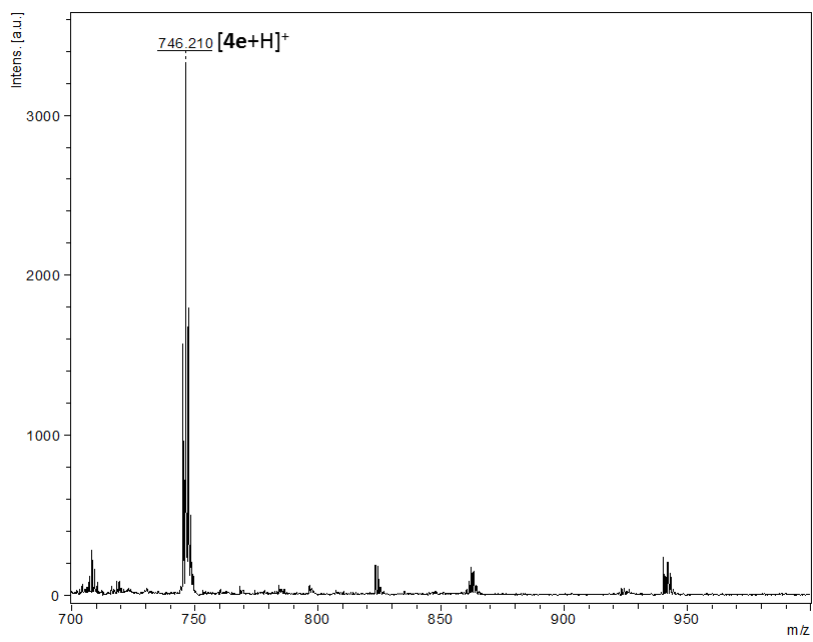


Figure 57_SM - MALDI-TOF mass spectra of compound **4e** after titration with 1 equiv. and 2 equiv. of $\text{Cd}(\text{BF}_4)_2 \cdot x\text{H}_2\text{O}$ (*dried-droplet method*).

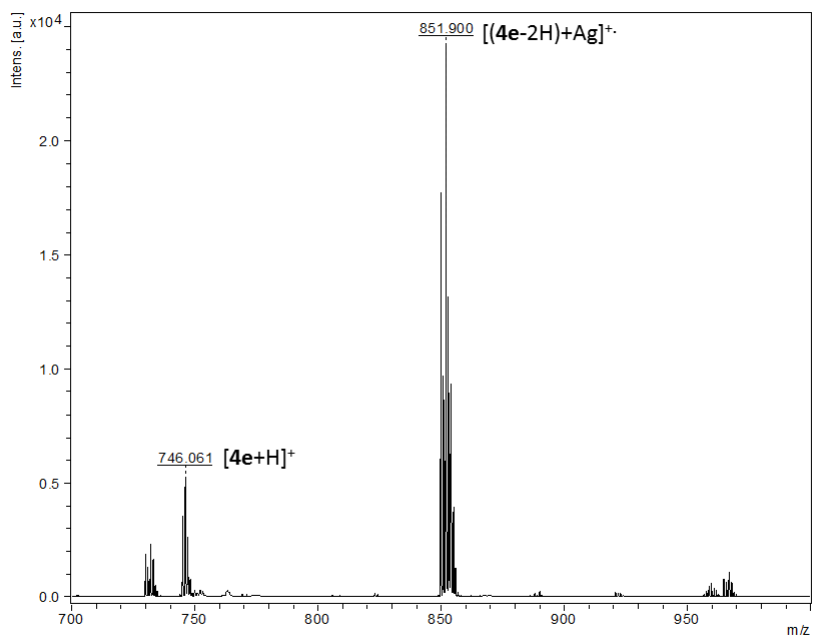
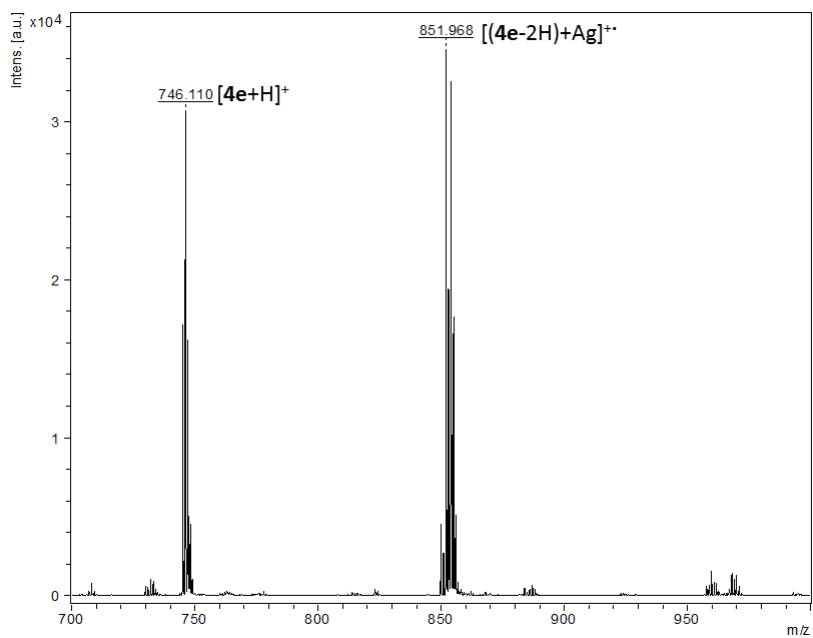


Figure 58_SM - MALDI-TOF mass spectra of compound **4e** after titration with 1 equiv. (above) and 2 equiv. of $Ag(BF_4)_xH_2O$ (below) (*dried-droplet method*).

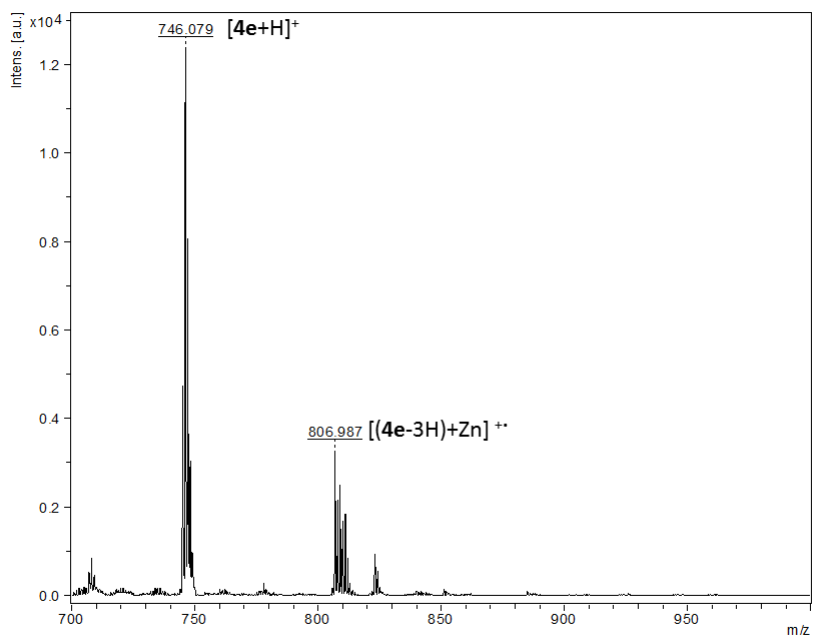


Figure 59_SM - MALDI-TOF mass spectra of compound **4e** after titration with of $\text{Zn}(\text{BF}_4)_2 \cdot x\text{H}_2\text{O}$ (*layer-by-layer method*).

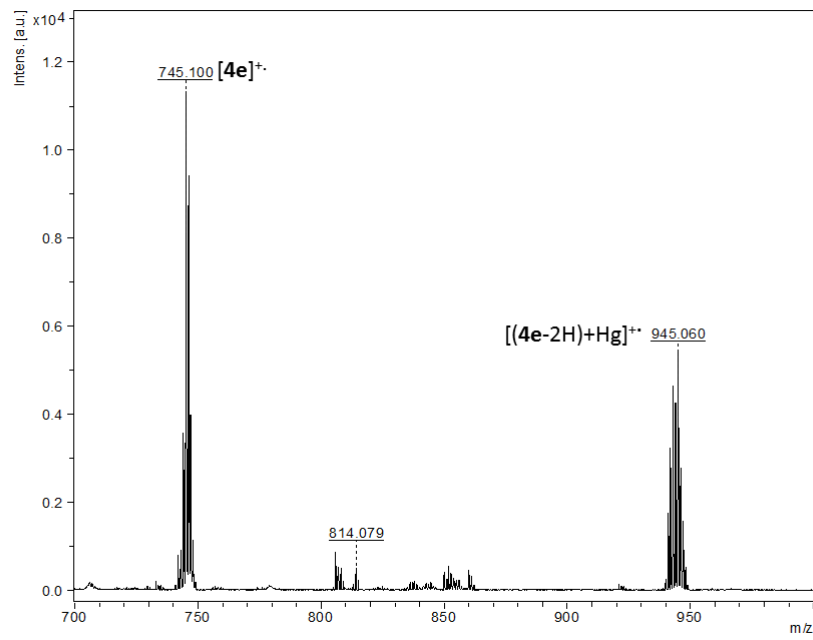


Figure 60_SM - MALDI-TOF mass spectra of compound **4e** after titration with of $\text{Hg}(\text{BF}_4)_2 \cdot x\text{H}_2\text{O}$ (*layer-by-layer method*).

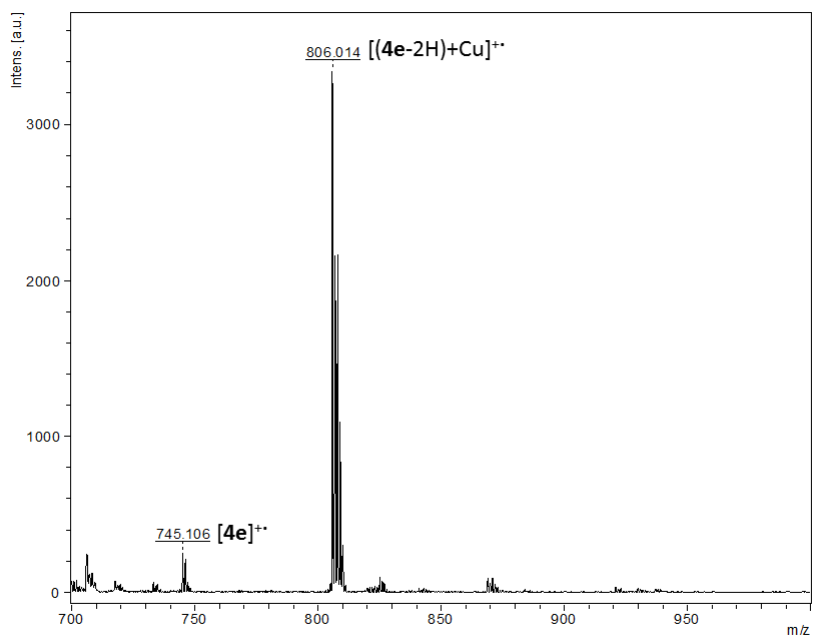


Figure 61_SM - MALDI-TOF mass spectra of compound **4e** after titration with of $\text{Cu}(\text{BF}_4)_2 \cdot x\text{H}_2\text{O}$ (*layer-by-layer method*).

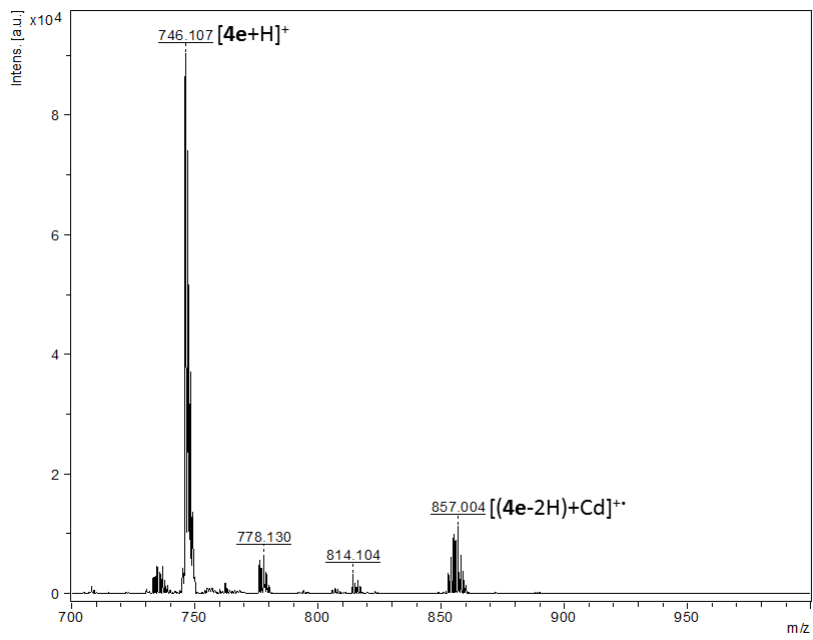


Figure 62_SM - MALDI-TOF mass spectra of compound **4e** after titration with of $\text{Cd}(\text{BF}_4)_2 \cdot x\text{H}_2\text{O}$ (*layer-by-layer method*).

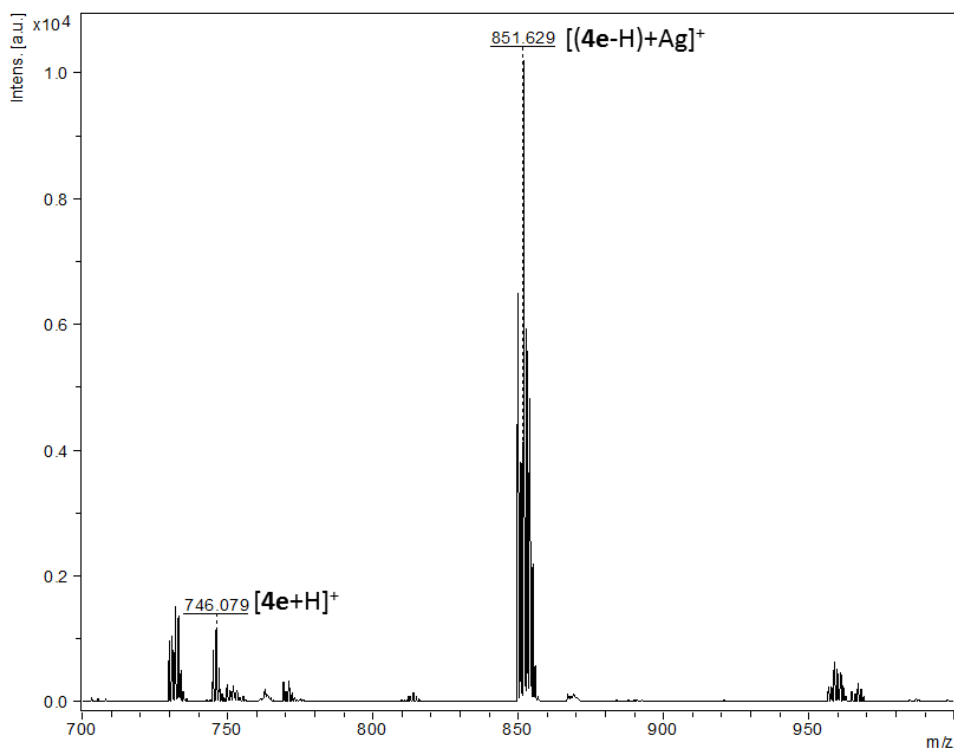


Figure 63_SM - MALDI-TOF mass spectra of compound **4e** after titration with of $\text{Ag}(\text{BF}_4)_x\text{H}_2\text{O}$ (*layer-by-layer method*).